

Relay Feedback Identification and Control for Smith Predictor Structure

An end-term report submitted in partial fulfilment of the requirements for the award of the degree in

Master of Technology
(Systems and Control Engineering)

Submitted by

MITHUN DAS

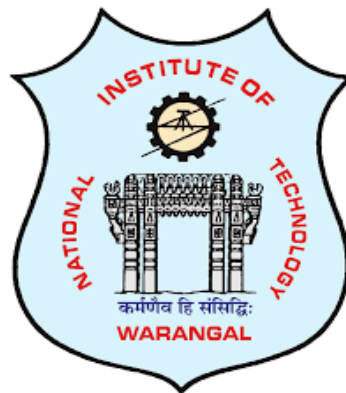
Roll No: 21CHM2R06

Department of Chemical Engineering

Under the guidance of

Prof. Anand Kishore Kola (supervisor)

Department of Chemical Engineering



DEPARTMENT OF CHEMICAL ENGINEERING

NATIONAL INSTITUTE OF TECHNOLOGY

506004

JUNE 2023

Dissertation Approval for M-Tech

This dissertation entitled **Relay Feedback Identification and Control for Smith Predictor Structure** by **Mithun Das** is approved for the degree of M-Tech in Systems & Control Engineering.

Examiners

Supervisor (s)

Chairman

Date: _____

Place: _____

CERTIFICATE

This is to certify that the progress work entitled "**Relay Feedback Identification and Control for Smith Predictor Structure**" is a bonafide record of work carried out by "**Mithun Das (21CHM2R06)**", submitted to the faculty of the Chemical Engineering Department, in partial fulfilment of the requirement for the award of the degree of **Master of Technology in Systems & Control Engineering** at National Institute of Technology, Warangal during the academic year 2022-2023.

Dr. P.V. Suresh

Head of the Department

Department of Chemical Engineering

NIT Warangal-50600

Prof. Anand Kishore Kola

Project Supervisor

Department of Chemical Engineering

NIT Warangal-50600

DECLARATION

I declare that this submission represents the implementation of my and my supervisor's ideas. The literature referred to has been appropriately cited and references the original sources. I affirm my adherence to the principles of academic honesty and integrity, without misrepresenting, fabricating, or falsifying any ideas, facts, data, or sources. I acknowledge that any violation of these guidelines may result in disciplinary actions by other institutions and potential penal consequences for uncredited or unauthorized use of sources.

(Signature)

Mithun Das

Roll No. 21CHM2R06

Date: _____

Acknowledgement

I would like to express my sincere gratitude to Prof. Anand Kishore Kola and Dr. Uday Bhaskar Babu Gara from the Department of Chemical Engineering for their unwavering trust, invaluable input, time, insights, and moral support throughout my project. Their guidance has been instrumental in my current work and will undoubtedly benefit me in the future.

Additionally, I extend my heartfelt appreciation to the Head of the Chemical Engineering Department at NIT Warangal for their exceptional encouragement, motivation, and generosity in providing the necessary facilities.

I am grateful to the entire department staff, who, despite their heavy workload, have always been willing to assist me.

Lastly, but most importantly, I would like to acknowledge the constant encouragement, support, and unwavering belief in me from my college friends and my parents. I am also grateful to NITW for providing me with an enriching platform that has helped me grow in every aspect.

Mithun Das
21CHM2R06

Abstract

This research focuses on identifying and controlling unknown processes using relay feedback and designing an Internal Model Control (IMC)-based PID controller in a Smith predictor configuration. The proposed method utilizes an asymmetric relay combined with a fractional-order integrator to accurately identify the process as First Order with Delay Time (FOPDT) and Critically-Damped Second Order with Delay Time (CSOPDT) models. The fractional integrator improves the accuracy of frequency measurements obtained using the Describing Function (DF) method. The identified process parameters can be calculated by deriving precise expressions for limit cycle frequency and amplitude. These identified models are then implemented in a fractional filler with IMC-based PID controllers to design the controllers. Performance evaluation is conducted based on criteria such as Integral of Absolute Error (IAE), Integral of Square Error (ISE), and Total Variation (TV), with simulations performed in MATLAB Simulink.

Contents

1.	Introduction	1
1.1	Relay Feedback	1
1.2	Smith predictor Structure	2
1.3	Feedback configuration with fractional filter	3
2.	Literature Review	4
2.1	Research Gaps	5
3.	Motivation and Objectives.....	6
3.1	Objectives	6
4.	Societal Application of the Project.....	7
5.	Proposed Methodology	8
5.1	Process identification	8
5.1.1	Critically damped SOPDT dynamics.....	9
5.1.2	FOPDT dynamics	10
5.2	Controller design	11
5.3.	Closed Loop Performance and Robustness Analysis	13
6.	Simulation Result and discussion	15
6.1	Example 1	15
6.1.1	Identification	15
6.1.2	Controller design	16
6.1.3	Robust Analysis.....	19
6.2	Example 2	24
6.2.1	Identification	24
6.2.2	Controller design	25
6.2.3	Robust Analysis.....	28
6.3	Example 3	33
6.3.1	Identification	33
6.3.2	Controller design	34
6.3.3	Robust Analysis.....	37
7.	Identification of HO Model & Control for Feedback Configurations	43
7.1	Identification of HO Models	43
7.2	Controller design	45
8.	Conclusion.....	48
9.	Future Work.....	49
10.	References	50

List of Figures

Fig. 1.1: Diagram of relay test	1
Fig. 1.2: Diagram of Limit Cycle	2
Fig. 1.3: Smith predictor configuration	2
Fig. 1.4: Fractional Filter with PID	3
Fig. 5.1: Block diagram of Relay feedback with FO integral.....	8
Fig. 5.2: Limit cycle	8
Fig. 5.3: Feedback control scheme	11
Fig. 6.1: Nyquist Plot of FOPDT for Example 1	15
Fig. 6.2: Nyquist Plot of SOPDT for Example 1	16
Fig. 6.3: Response for example 1 FOPDT Process	18
Fig. 6.4: Response for example 1 SOPDT Process	18
Fig. 6.5: Response of ex.1 for + - 10%, + - 20% change in Time Delay for FOPDT Known Gain	20
Fig. 6.6: Norm-bound uncertainty of Example 1 for FOPDT Known Gain	20
Fig. 6.7: Response of ex.1 for +/- 10%, +/- 20% change in Time Delay for FOPDT Calculated Gain	21
Fig. 6.8: Norm-bound uncertainty of Example 1 for FOPDT Calculated Gain.....	21
Fig. 6.9: Response of ex.1 for +/- 10%, +/- 20% change in Time Delay for SOPDT Known Gain.....	22
Fig. 6.10: Norm-bound uncertainty of Example 1 for SOPDT Known Gain.....	22
Fig. 6.11: Response of ex.1 for +/- 10%, +/- 20% change in Time Delay for SOPDT Calculated Gain	23
Fig. 6.12: Norm-bound uncertainty of Example 1 for SOPDT Calculated Gain.....	23
Fig. 6.13: Nyquist Plot of FOPDT for Example 2.....	24
Fig. 6.14: Nyquist Plot of SOPDT for Example 2.....	25
Fig. 6.15: Response of ex.2 FOPDT Process	27
Fig. 6.16 : Response of ex.2 SOPDT Process	27
Fig. 6.17: Response of ex.2 for +/- 10%, +/- 20% change in Time Delay for FOPDT Known Gain.....	29
Fig. 6.18: Norm-bound uncertainty of Example 2 for FOPDT Known Gain	29
Fig. 6.19: Response of ex.2 for +/- 10%, +/- 20% change in Time Delay for FOPDT Calculated Gain	30
Fig. 6.20: Norm-bound uncertainty of Example 2 for FOPDT Calculated Gain.....	30
Fig. 6.21: Response of ex.2 for +/- 10%, +/- 20% change in Time Delay for SOPDT Known Gain.....	31
Fig. 6.22: Norm-bound uncertainty of Example 2 for SOPDT Known Gain	31
Fig. 6.23: Response of ex.2 for +/- 10%, +/- 20% change in Time Delay for SOPDT Calculated Gain	32
Fig. 6.24: Norm-bound uncertainty of Example 2 for SOPDT Calculated Gain.....	32
Fig. 6.25: Nyquist Plot of FOPDT for Example 3.....	34
Fig. 6.26: Nyquist Plot of SOPDT for Example 3.....	34
Fig. 6.27: Response of ex. 3 FOPDT Process	36
Fig. 6.28: Response of ex. 3 FOPDT Process	37
Fig. 6.29: Response of ex.3 for +/- 10%, +/- 20% change in Time Delay for FOPDT Known Gain.....	38
Fig. 6.30: Norm-bound uncertainty of Example 3 for FOPDT Known Gain	39
Fig. 6.31: Response of ex.1 for +/- 10%, +/- 20% change in Time Delay for FOPDT Calculated Gain	39
Fig. 6.32: Norm-bound uncertainty of Example 3 for FOPDT Calculated Gain.....	40
Fig. 6.33: Response of ex.3 for +/- 10%, +/- 20% change in Time Delay for SOPDT Known Gain.....	40
Fig. 6.34: Norm-bound uncertainty of Example 3 for SOPDT Known Gain	41
Fig. 6.35: Response of ex.3 for +/- 10%, +/- 20% change in Time Delay for SOPDT Calculated Gain	41
Fig. 6.36: Norm-bound uncertainty of Example 1 for SOPDT Calculated Gain.....	42
Fig. 7.1: Set-point unit step response for process example 1	46
Fig. 7.2: Set-point unit step response for process example 2	46
Fig. 7.3: Set-point unit step response for process example 4	46
Fig. 7.4: Set-point unit step response for process example 5	47
Fig. 7.5: Set-point unit step response for process example 6	47

List of Tables

Table 6.1: Comparison of proposed models Example 1	15
Table 6.2: Comparison of filters Example 1	17
Table 6.3: Comparison of IAE, ISE and TV Example 1	17
Table 6.4: Performance Criteria for Perturbations in Process Model (Example 1)	19
Table 6.5: Comparison of proposed models Example 2	24
Table 6.6: Comparison of filters Example 2	26
Table 6.7: Comparison of IAE, ISE and TV Example 2	26
Table 6.8: Performance Criteria for Perturbations in Process Model (Example 2)	28
Table 6.9: Comparison of proposed models Example 3	33
Table 6.10: Comparison of filters Example 3	35
Table 6.11: Comparison of IAE, ISE and TV Example 3	36
Table 6.12: Performance Criteria for Perturbations in Process Model (Example 3)	37
Table 7.1: Parameters of the identified CSOPDT model	43
Table 7.2: Comparison of process models	44
Table 7.3: Controller Design of Identified Higher Order Models	45

Abbreviations

Abbreviations	Definitions
FOPDT	First Order plus Delay Time
SOPDT	Second Order plus with Delay Time
CSOPDT	Critically-Damped Second Order with Delay
DF	Describing Function
IMC	Internal Model Control
PID	Proportional Integral Derivative
TV	Total Variations
IAE	Integral of Absolute Error
ISE	Integral of Square Error
ZN	Ziegler Nichols
FO	First order
HO	Higher order
SR	Symmetrical Relay
AR	Asymmetrical Relay
R	Approximate Gain of Relay
$G_p(s)$	Unknown process
$G_c(s)$	Controller
N	Cascade combination of integrator and relay
$y(sp)$	Set Point
$y(t)$	Process Output
$u(t)$	Process Input
$e(t)$	Error Signal
$v(t)$	Relay Input Signal
A	Peak Amplitude Of Relay
ω	Fundamental Frequency
$r(t)$	Process Output Signal
ϵ	Asymmetrical Relay With Hysteresis
τ	Time Constant
θ	Process Delay
k	Calculated Gain of Process
α	Fractional order
D	Disturbance
γ	Filter Time Constant
p	Filter Order.
T	Time Period of Process through relay test
T_u	Time Period of Process from margin
h	Height of Relay
A_p	Maximum Overshoot
A_v	Maximum undershoot
int-F-KG	Integer First Order Known Gain
int-F-CG	Integer First Order Calculated Gain
fra-F-KG	Fractional First Order Known Gain
fra-F-CG	Fractional First Order Calculated Gain
int-S-KG	Integer Second Order Known Gain
int-S-CG	Integer Second Order Calculated Gain
fra-S-KG	Fractional Second Order Known Gain
fra-S-CG	Fractional Second Order Calculated Gain

1. Introduction

PID controllers are widespread in process industries, and accurate process model identification plays a crucial role in their tuning. Process models can be identified through open-loop and closed-loop methods. While open-loop identification involves individual excitation of process inputs and observing the corresponding output responses, drawbacks include sensitivity to disturbances, increased computational time, and occasional deviations from the set point. In contrast, closed-loop identification methods overcome these limitations.

Relay feedback identification, a closed-loop testing method, has gained attention for PID controller tuning due to its simplicity. By employing a relay in the feedback loop, sustained oscillations known as a limit cycle are generated. These limit cycles provide valuable process information, such as peak amplitude and ultimate frequency, which can be used to obtain the process model parameters.

Different controller design methods have been proposed for set point tracking and disturbance rejection. IMC-based methods incorporate set point weighting and filtering to suppress overshoot and ensure better closed-loop performance. The design of an IMC-PID controller for SOPDT processes using a fractional IMC filter has shown promising results. This research paper focuses on the identification of processes using the relay feedback method and the design of an IMC-PID controller with a fractional IMC filter in a Smith predictor configuration. The effectiveness of the proposed method is demonstrated through simulations based on examples from a reference paper [17], using MATLAB and Simulink. The fractional filter term is determined based on the identified model's time delay and gain margin, aiming for a faster closed-loop response. In order to obtain faster closed loop response, the Proportional term has been divided by a constant κ which varies from $0.2 < \kappa < 1$. The resulting controller structure consists of a PID controller in series with a fractional filter, and the closed-loop performance is evaluated using ISE and IAE metrics.

1.1 Relay Feedback

The relay feedback method provides an efficient and time-effective way to identify and process information around the critical frequency, known as the ultimate frequency, $\omega = \frac{2\pi}{P_u}$. A relay is an electrically operated switch. Relays are divided into two types, Symmetrical Relay and Asymmetrical Relay. It ensures that the process does not deviate significantly from the nominal operating point and is particularly useful for processes with large time constants. The relay generates sustained oscillations by maintaining the proportional gain above a certain value, facilitating process model identification. Identification can be made in time and frequency domain. Accurate dynamics models help in estimating the controller parameter.

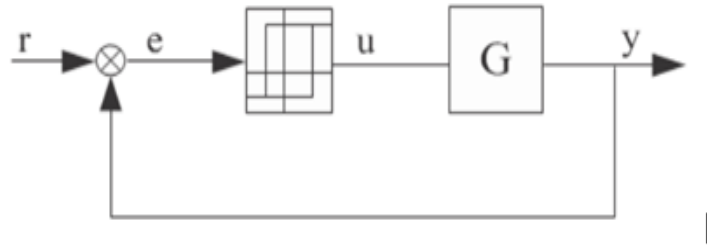


Fig. 1.1: Diagram of relay test

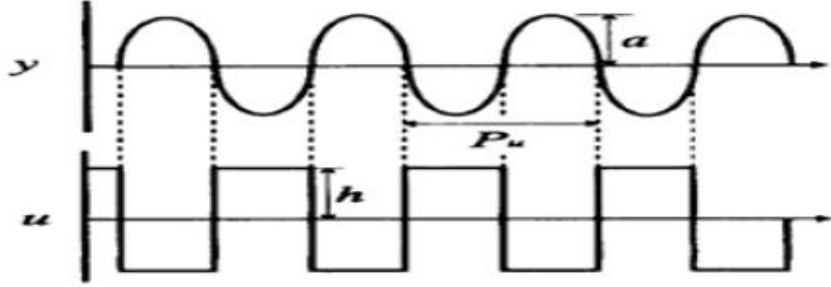


Fig. 1.2: Diagram of Limit Cycle

Online identification involves the simultaneous estimation of model parameters and controller adjustments, while offline identification focuses solely on estimating model parameters without controller involvement.

1.2 Smith predictor Structure

The Smith predictor, designed for systems with significant feedback time delays, serves as a dead-time compensator for stable processes with long delays. The main concept underlying the Smith predictor (refer to Fig. 1.3) is to anticipate the actual process output using a transfer function representing the process model. When the predicted output aligns with the actual process output, the control signal is derived from the plant model, excluding any delay term. This approach ensures that the controller action remains unaffected by time delay, leading to a significant improvement in control performance.

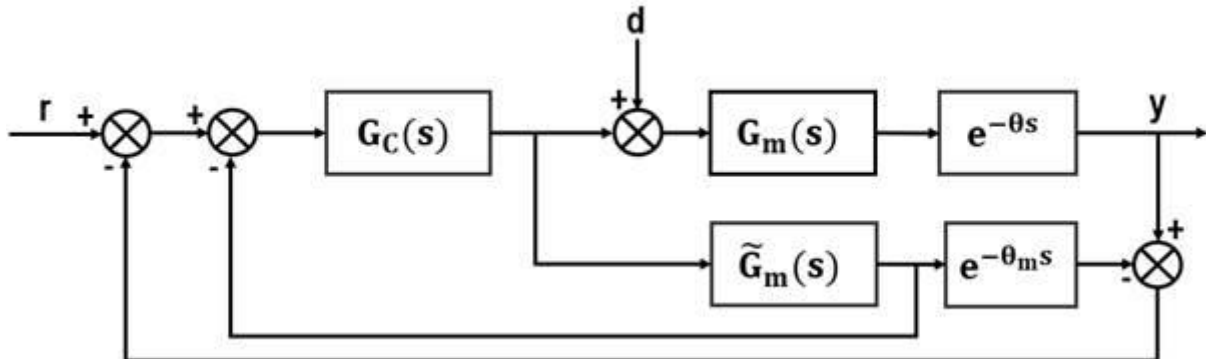


Fig. 1.3: Smith predictor configuration

According to the provided equation (1), the transfer function of the Smith predictor, denoted as

$$T_{\text{smith}}(s) = \frac{G_C(s) G_m e^{-\theta s}}{1 + G_C(s) G_m(s)} \quad (1)$$

This equation shows that the parameters of the controller, $G_C(s)$, often chosen as PI or PID, can be determined by considering a model of the delay-free component of the plant.

1.3 Feedback configuration with fractional filter

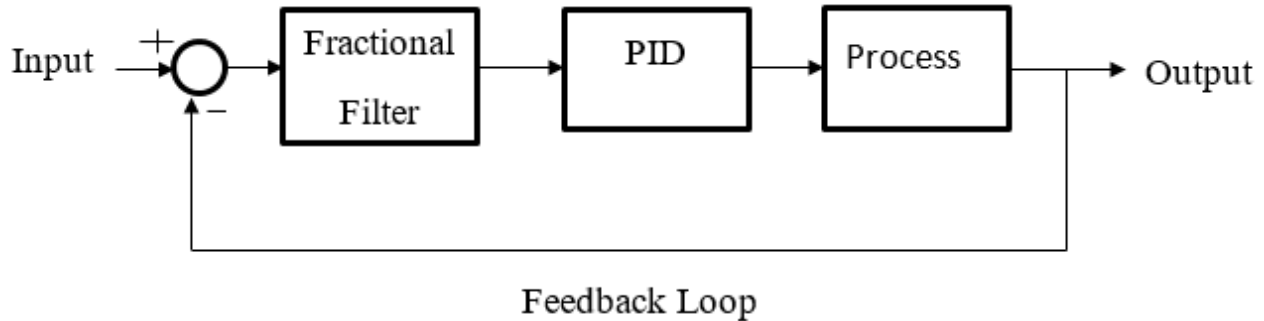


Fig. 1.4: Fractional Filter with PID

Importance of Fractional Filter

1. The utilization of a fractional-order filter proves to be effective in attenuating high-frequency noise and enhancing the precision of the feedback signal. Incorporating a fractional-order filter in the system leads to improved control and stability, minimizing overshoot, undershoot, and settling time.
2. A fractional-order filter employs a fractional-order differential equation to filter signals, with the order of the filter ranging between 0 and 1.1. When combined with a PID controller within a feedback control system, a fractional-order filter facilitates more accurate and stable control of the system.
3. Enhancing the performance of a PID controller can be accomplished by applying a fractional filter to shape the input signal before it reaches the PID controller. This approach contributes to improved control accuracy and stability in the system.

2. Literature Review

A literature review was conducted to explore the relay feedback identification technique and controller design for the Smith predictor structure. The initial use of the relay feedback method was to design PID tuning based on the ultimate period and amplitude of the process [1]. The identification of a second-order plus time delay (SOPDT) process was achieved by applying an asymmetrical relay test and using the Laplace transform of the process input-output signals [2]. The identification accuracy was improved by employing a symmetrical relay test [3].

For non-minimum phase systems, a method capable of identifying process models with a maximum of four parameters was reported. To handle measurement noise at the system output, a curve fitting method was used to recover noise-free limit cycles [4]. Identification of the SOPDT model to FOPDT model was performed both online and offline using DF method [5]. The asymmetrical relay test was employed to identify the HO process as FOPDT, CSOPDT (complex SOPDT models with repeated poles for a non-zero set point [6]. Mathematical expressions were derived using the state space method to estimate unknown process parameters [7]. Unknown processes were identified as CSOPDT models using fractional step test data [8].

A new method called the shift method was proposed for identifying unknown processes. Three points on the process frequency response plot were estimated, and based on these points and an optimization technique, the SOPDT process model was identified [9]. Analytical expressions were developed for identifying the SOPDT process model using the shift method [10]. Additional delay and an integrator were introduced into the relay feedback loop to improve the position on the frequency response curve for accurate identification [11] [12]. The shift technique was extended for the identification of integrating and unstable processes, utilizing a filter called the shift filter to estimate the next point on the process frequency response [13]. Identification of higher-order liquid level processes as FOPDT and SOPDT models was performed [14]. Ideal relay was used in MATLAB Simulink as well as real-time liquid level processes for identification and control [15].

The PID controller has been widely used in industrial applications for centuries due to its simple structure and available tuning rules [16]. However, tuning methods for PID controllers are still evolving to improve the closed-loop performance of processes that are associated with time delays, external perturbations, and nonlinearities [16]. The effectiveness of the present method was illustrated through simulations based on a reference paper [17]. Real processes need to be approximated as lower-order models to apply PID tuning rules [18]. Disturbance rejection can be achieved through direct synthesis by PI/PID controller design [19]. Improved auto-tuning schemes for PID controllers have been proposed [20]. SOPDT models provide better representation of process dynamics compared to FOPDT models [21]. The number of PID tuning rules for SOPDT processes is generally fewer [22] than for FOPDT processes [23].

The direct synthesis (DS) method and IMC schemes are commonly used for designing controllers for SOPDT processes [24]. Multi-variable feedback design has been employed [25]. Optimal tuning of PID controllers has been investigated for FOPDT, SOPDT, and SOPDT with lead processes [26]. DS controllers are designed based on the desired trajectory of the closed-loop transfer function, but they do not necessarily result in a PID form of the controller. DS controllers are suitable for set-point tracking but may not provide satisfactory performance for disturbance rejection. IMC-based designs

yield a PID controller structure through proper approximation of the process model. Several controller tuning methods based on the IMC-PID method have been proposed for SOPDT processes, including robust process control selection [27] and PID tuning rules for SOPDT systems [28]. This work focuses on process identification using the proposed relay feedback method and the design of an IMC-PID controller using a fractional IMC filter for Smith predictor configurations [29].

2.1 Research Gaps

1. There is no considerable work on the combination of Relay with Fractional Integrator for system Identification.
2. There are no useful techniques to identify Higher Order (HO) systems.
3. Less studies have been performed to reduce the Total Variation (TV) value after tuning the controller.

3. Motivation and Objectives

Relay feedback identification is a powerful technique for parameter estimation in control systems, especially when direct measurement is challenging. It involves introducing periodic perturbations to the system input and analysing the resulting output to extract information about system parameters such as gain, time constant, and delay.

The combination of relay feedback identification and control is particularly effective in systems with long delays, such as those found in Smith Predictor configurations. The Smith Predictor is commonly used for systems with significant time delays but can be difficult to tune and may exhibit instability. By utilizing relay feedback identification and control, it is possible to enhance the stability and performance of Smith Predictor configurations.

Even in simple feedback configurations, which are the most prevalent type of control system, relay feedback identification and control can yield advantages. Accurate identification of system parameters and the use of relay feedback control can lead to enhanced performance and stability compared to traditional PID controllers.

The proposal to employ relay feedback identification and control in these various control configurations aims to enhance performance, stability, and robustness, particularly in systems with long delays or nonlinear characteristics.

3.1 Objectives

1. To identify a model using relay feedback with fractional integrator for smith predictor structures (completed)
2. To design fractional order IMC PID controller for smith predictor structures. (completed)
3. To identify HO model using relay feedback with fractional integrator for simple feedback structures (completed).
4. To design fractional order IMC PID controller for simple feedback structures (completed).

4. Societal Application of the Project

1. Relay feedback identification and control can be implemented in ADAS systems to enhance the control of the vehicle's suspension system. The suspension system plays a crucial role in maintaining vehicle stability and handling, especially during maneuvers and cornering. By employing relay feedback identification and control, the performance and stability of the suspension system can be improved, leading to enhanced vehicle handling and a reduced risk of accidents.
2. The control of the vehicle's braking system is another potential application of relay feedback identification and control in ADAS systems. Braking systems are critical for ensuring safe vehicle operation, particularly in emergency situations. By utilizing relay feedback identification and control, the performance and stability of the braking system can be enhanced, resulting in improved stopping distance and a decreased risk of accidents.
3. Process control in industrial applications stands as a significant area where relay feedback identification and control can find valuable applications. Industrial processes extensively utilize control systems to regulate various variables, including flow rate, pressure and temperature. By enhancing the performance and stability of control systems through relay feedback identification and control, the efficiency of these processes can be increased, leading to reduced waste and energy consumption.
4. Robotics represents another potential field where this project's applications are relevant. Precise control over robot movements and interactions with the environment is crucial for robotic systems. By incorporating relay feedback identification and control, the precision and accuracy of robotic control systems can be improved, paving the way for the development of more advanced and capable robots for diverse applications, including manufacturing, healthcare, and space exploration.
5. The project's potential applications extend to the field of renewable energy. Control systems play a vital role in regulating the output of renewable energy sources like solar panels and wind turbines. By enhancing the performance and stability of these control systems through relay feedback identification and control, the efficiency of renewable energy production can be increased, leading to lower energy costs for consumers.

Overall, the societal applications of this project are numerous and varied, and include improvements in industrial processes, robotics, renewable energy, and many other fields that rely on precise and stable control systems.

5. Proposed Methodology

5.1 Process identification

The relay feedback identification scheme is used to identify the HO process model as a CSOPDT model. The unknown process $G_p(s)$ is to be identified using an asymmetrical relay R and a fractional order integral with order α . The cascade combination of an integrator and relay is represented by the block diagram in Fig. 5.1. The process generates sustained oscillations, also known as a limit cycle, as shown in Fig. 5.2. The relay input is denoted by $u(t)$, the process output by $y(t)$, the set point by $r(t)$, the error signal by $e(t)$, and the relay input signal by $v(t)$.

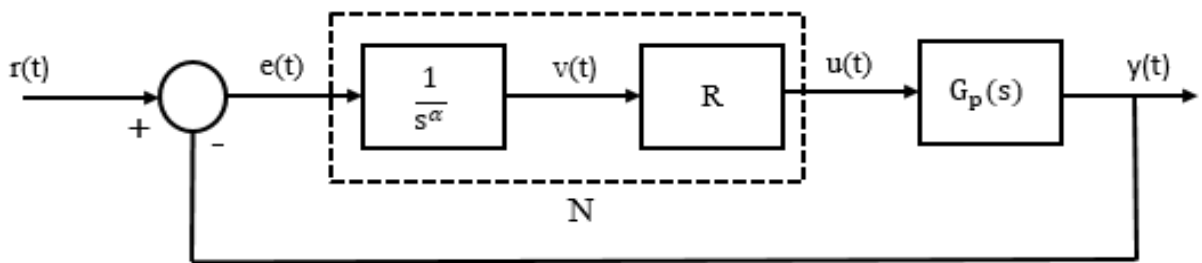


Fig. 5.1: Block diagram of Relay feedback with FO integral

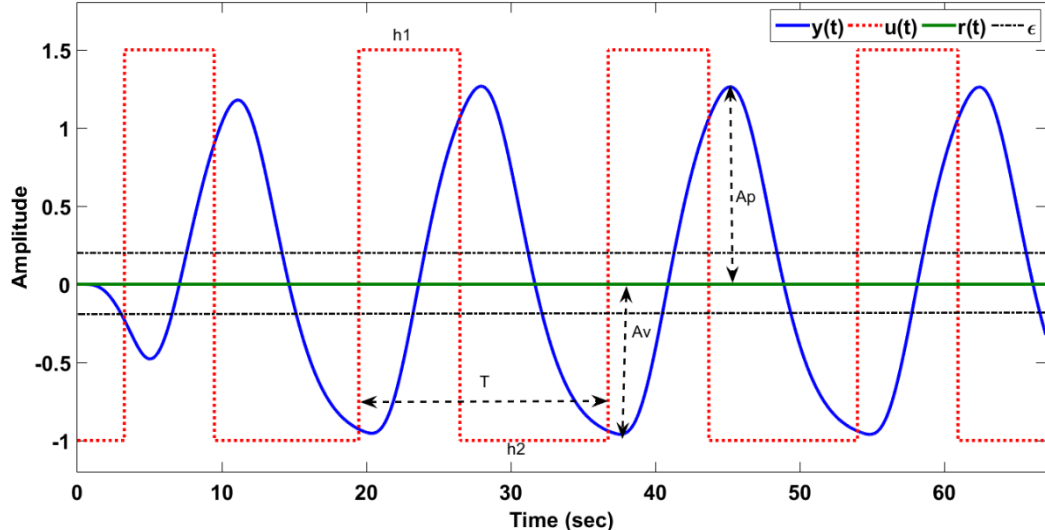


Fig. 5.2: Limit cycle

$$e(t) = A \sin(\omega t) \quad (2)$$

The error signal $e(t)$ is defined as $A \sin(\omega t)$, where A is the peak amplitude of the relay input signal and ω is the fundamental frequency of the process output signal when $r(t)$ is set to zero. The fractional order integral follows the Riemann-Liouville (R-L) definition [6] and can be expressed as

$$\frac{1}{s^\alpha} = \frac{1}{(j\omega)^\alpha} = e^{-j\frac{\pi}{2}\alpha} \quad (3)$$

The relay gain R, which approximates the gain of the switching element, is derived using the DF method [16]. The expression for R of the set-point weighted asymmetrical relay with hysteresis (ϵ) is modified and given by

$$R = \frac{2(h_1+h_2)\sqrt{A_m^2\left(1-\left(\frac{B}{A_m}\right)^2\right)-\epsilon^2-j\epsilon}}{\pi A_m^2} \quad (4)$$

The DF of the relay with the fractional order integral is denoted as N and is represented by Equation 5. The parameters Am, B, h1, and h2 are defined as shown in Equations 6 and 7.

$$N = \frac{2(h_1+h_2)\sqrt{A_m^2\left(1-\left(\frac{B}{A_m}\right)^2\right)-\epsilon^2-j\epsilon}}{\pi A_m^2} e^{-j\frac{\pi}{2}\alpha} \quad (5)$$

$$A_m = \frac{A_p + A_v}{2} \quad (6)$$

$$B = |A_m - A_p| \quad (7)$$

Where N is DF of Relay with FO integral, h1 and h2 are relay Amplitudes with hysteresis ϵ , A_p and A_v positive and negative amplitudes of $y(t)$. The condition to obtain sustained oscillations during identification is

$$NG_p(j\omega) = -1 \quad (8)$$

5.1.1 Critically damped SOPDT dynamics

Consider the following CSOPDT process model in the Laplace domain as

$$G_p(s) = \frac{ke^{-\theta s}}{(\tau s + 1)^2} \quad (9)$$

In the frequency domain, $s = j\omega$

$$G_p(j\omega) = \frac{ke^{-\theta j\omega}}{(\tau j\omega + 1)^2} \quad (10)$$

In the case of a CSOPDT process, the process model in the Laplace domain is represented by Equation 9. By substituting Equation 10 and Equation 5 into Equation 8, the magnitude and phase angle equations can be derived to estimate the time constant (τ) and the delay (θ) of the process (Equations 11-15).

$$\frac{ke^{-\theta j\omega} 2(h_1+h_2) \sqrt{A_m^2 \left(1 - \left(\frac{B}{A_m}\right)^2\right) - \epsilon^2 - j\epsilon}}{(\tau j\omega + 1)^2 \pi A_m^2} e^{-j\frac{\pi}{2}x} = -1 \quad (11)$$

Now equate the magnitude on both sides of the above equation (11) and solve for the Time constant as

$$\tau = \frac{1}{\omega} \sqrt{\left(\frac{2k(h_1+h_2) \sqrt{\left(1 - \left(\frac{B}{A_m}\right)^2\right)}}{\pi A_m} \right)^2 - 1} \quad (12)$$

Now equating the phase angle of both sides Phase of equation (12) and simplifying for process Delay

$$\theta = \frac{1}{\omega} \left[F - \tan^{-1} \left(\frac{\epsilon}{x} \right) - 2 \tan^{-1} (\tau \omega) \right] \quad (13)$$

Where

$$F = \pi - x \frac{\pi}{2} \quad (14)$$

$$x = \sqrt{A_m^2 \left(1 - \left(\frac{B}{A_m}\right)^2\right) - \epsilon^2} \quad (15)$$

$$k = \frac{\int_t^{t+T} y(t) dt}{\int_t^{t+T} u(t) dt} \quad (16)$$

5.1.2 FOPDT dynamics

Consider the following FOPDT process model in the Laplace domain as

$$G_p(s) = \frac{ke^{-\theta s}}{(ts+1)} \quad (17)$$

In the frequency domain, $s = j\omega$

$$G_p(j\omega) = \frac{ke^{-\theta j\omega}}{(\tau j\omega + 1)} \quad (18)$$

For a FOPDT process, the process model in the Laplace domain is represented by Equation 17. By substituting Equation 18 and Equation 5 into Equation 8, the magnitude and phase angle equations can be derived to estimate the time constant (τ) and the delay (θ) of the process (Equations 19-21).

$$\frac{ke^{-\theta j\omega} 2(h_1+h_2) \sqrt{A_m^2 \left(1 - \left(\frac{B}{A_m}\right)^2\right) - \epsilon^2 - j\epsilon}}{(\tau j\omega + 1)^2 \pi A_m^2} e^{-j\frac{\pi}{2}x} = -1 \quad (19)$$

Now equate the magnitude on both sides of the above equation (19) and solve for the Time constant as

$$\tau = \frac{1}{\omega} \sqrt{\left(\left[\frac{2k(h_1+h_2)\left(1-\left(\frac{B}{A_m}\right)^2\right)}{\pi} \right]^2 - 1 \right)} \quad (20)$$

Now equating the phase angle of both sides Phase of equation (11) as and simplifying for process Delay

$$\theta = \frac{1}{\omega} \left[F - \tan^{-1} \left(\frac{\varepsilon}{x} \right) - \tan^{-1} (\tau \omega) \right] \quad (21)$$

To estimate the unknown parameters of the CSOPDT process, Equations 12, 13, and 16 are used. For the FOPDT process, Equations 20, 21, and 16 are used to estimate the process time constant, delay, and gain, respectively. These equations provide a framework for identifying the CSOPDT and FOPDT process models using the relay feedback identification scheme and the fractional order integral.

5.2 Controller design

The feedback control scheme shown in Figure 3 includes $G_p(s)$, G_C , and the IMC controller. The variables $y_{sp}(t)$, $y(s)$, p , and D represent the set point, controlled variable, control input, and disturbance, respectively. The controller design using the fractional filter IMC method is as follows:

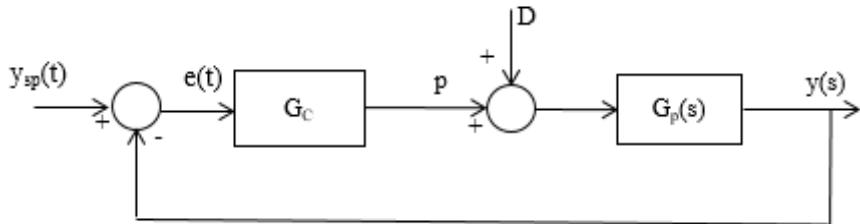


Fig. 5.3: Feedback control scheme

Decompose the process model into non-invertible and invertible parts. $\check{G}^+(s)$ represents the non-invertible part containing time delays and unstable zeros, while $\check{G}^-(s)$ represents the invertible part containing minimum phase elements. The IMC controller is given by:

$$G_{IMC}(s) = \frac{f(s)}{\check{G}^-(s)} \quad (22)$$

Where $f(s)$ is the IMC filter. The feedback controller is:

$$G_c(s) = \frac{G_{IMC}(s)}{1 - G_{IMC}(s)\tilde{G}(s)} \quad (23)$$

The proposed IMC controller scheme is:

$$G_c(s) = (\text{Filter}) \left[k_c \left(1 + \frac{1}{\tau_i s} + \tau_d s \right) \right] \quad (24)$$

Consider a CSOPDT model given by:

$$G(s) = \frac{k e^{-\theta s}}{(\tau s + 1)^2} \quad (25)$$

Where k is the system gain, θ is the time delay, and τ is the process time constant. The filter used is:

$$f(s) = \frac{1}{\gamma s^p + 1} \quad (26)$$

Where γ is the filter time constant and p is the filter order. The IMC controller according to Equation (22) is:

$$G_{IMC}(s) = \frac{1}{\gamma s^p + 1} \frac{(\tau s + 1)^2}{k} \quad (27)$$

Finally, the IMC-PID controller using Equations (24), (26), and (28) is:

$$G_c(s) = \frac{(\tau s + 1)^2}{k} \frac{1}{[(\gamma s^p + 1) - e^{-\theta s}]} \quad (28)$$

The delay $e^{-\theta s}$ is expressed as a first-order fraction using Pade's rule. Now, the controller becomes:

$$G_c(s) = \frac{(\tau s + 1)^2}{k} \frac{1}{\left[(\gamma s^p + 1) - \frac{(1 - 0.5\theta s)}{(1 + 0.5\theta s)} \right]} \quad (29)$$

The above equation is simplified and compared with the controller settings:

$$G_c(s) = \left[\frac{0.5\theta s + 1}{0.5\gamma\theta s^p + \gamma + \theta} \right] \frac{2\tau}{k} \left(1 + \frac{1}{2\tau s} + \frac{\tau}{2} s \right) \quad (30)$$

$$G_c(s) = \left[\frac{0.5\theta s + 1}{0.5\gamma\theta s^p + \gamma s^{p-1} + \theta} \right] \frac{2\tau}{k} \left(1 + \frac{1}{2\tau s} + \frac{\tau}{2} s \right) \quad (31)$$

Equations (30) and (31) represent the controller for CSOPDT processes with integer order and fractional order, respectively. Similarly, the IMC-PID controller for FOPDT process models is given by:

$$G_c(s) = \left[\frac{0.5\theta s + 1}{0.5\gamma\theta s^p + \gamma + \theta} \right] \frac{\tau}{k} \left(1 + \frac{1}{\tau s} \right) \quad (32)$$

$$G_c(s) = \left[\frac{0.5\theta s + 1}{0.5\gamma\theta s^p + \gamma s^{p-1} + \theta} \right] \frac{\tau}{k} \left(1 + \frac{1}{\tau s} \right) \quad (33)$$

Equations (32) and (33) represent the controller for FOPDT processes with integer order and fractional order, respectively.

5.3. Closed Loop Performance and Robustness Analysis

The system identification and controller design methodology are described in section 2. The performance is also evaluated for variations in process parameters, using IAE, TV, and ISE formulas to assess system performance (Eq. 34-36).

$$\text{IAE} = \int_0^\infty |e(t)| dt \quad (34)$$

$$\text{TV} = \sum_{i=0}^{\infty} |u_{i+1} - u_i| \quad (35)$$

$$\text{ISE} = \int_0^\infty e^2(t) dt \quad (36)$$

Robustness is always the primary concern in process control because models used for controller design are typically inaccurate, and the characteristics of physical systems change with operating conditions and time. These conditions often lead to control systems deviating from the design specifications, rendering them ineffective. Therefore, it is crucial to design a controller that ensures the resilience of the closed-loop system against modelling errors and changes in process dynamics.

The robust stability condition, as stated in [37], is:

$$\|L_m(j\omega)T(j\omega)\| < 1 \quad \text{where } \omega \in (-\infty, \infty) \quad (37)$$

Where T (complementary sensitivity function) and 1 (bound on the process multiplicative uncertainty) are defined in eq. (38)

$$T(s)_{s=j\omega} = \frac{G_p(s)G_C(s)}{1+G_p(s)G_C(s)}; \quad l_m(j\omega) = \left| \frac{G_p(j\omega)-G_m(j\omega)}{G_m(j\omega)} \right| \quad (38)$$

The robust condition to be satisfied for uncertainty in θ

$$\|T(j\omega)\|_\infty < \frac{1}{|e^{-\Delta\theta}-1|} \quad (39)$$

All three examples are analysed by considering the uncertainty in θ and how the proposed controllers respond to the uncertainty in time delay.

6. Simulation Result and discussion

6.1 Example 1

$$G_1(s) = \frac{e^{-10s}}{(17s + 1)(6s + 1)}$$

6.1.1 Identification

A relay with parameters $h_1 = 1.5$, $h_2 = -1$, $\varepsilon = \pm 0.025$, and $\alpha = 0.1$ to 1.8 is applied to the system to generate a limit cycle. The data is chosen based on minimum IAE and ISE criteria. The measured limit cycle information for the FOPDT known gain is $\alpha = 0.1$, $A_P = 0.6922$, $A_v = 0.5129$, and $T = 52.67$. For the FOPDT calculated gain at $\alpha = 0.1$, $A_P = 0.6922$, $A_v = 0.5129$, and $T = 52.67$. The SOPDT known gain is $\alpha = 0.7$, $A_P = 1.0635$, $A_v = 0.8259$, and the corresponding $T = 88.5657$, while the SOPDT calculated gain is $\alpha = 0.3$, $A_P = 0.7881$, $A_v = 0.6305$, and $T = 61.69$.

The identified process models (refers to Table 6.1) are compared with the actual models and methods presented in the literature based on IAE and Nyquist plots.

Table 6.1: Comparison of proposed models Example 1

α	METHODS	MODEL	IAE
	Actual process	$\frac{e^{-10s}}{(17s + 1)(6s + 1)}$	--
0.1	FOPDT Known gain	$\frac{e^{-14.794s}}{(20.229s + 1)}$	0.0052
0.1	FOPDT Calculated gain	$\frac{1.0109e^{-14.756s}}{(20.487s + 1)}$	0.0053
0.7	SOPDT Known gain	$\frac{e^{-9.0567 s}}{(11.549s + 1)^2}$	0.0043
0.3	SOPDT Calculated gain	$\frac{1.0495e^{-9.0156s}}{(11.367s + 1)^2}$	0.0080

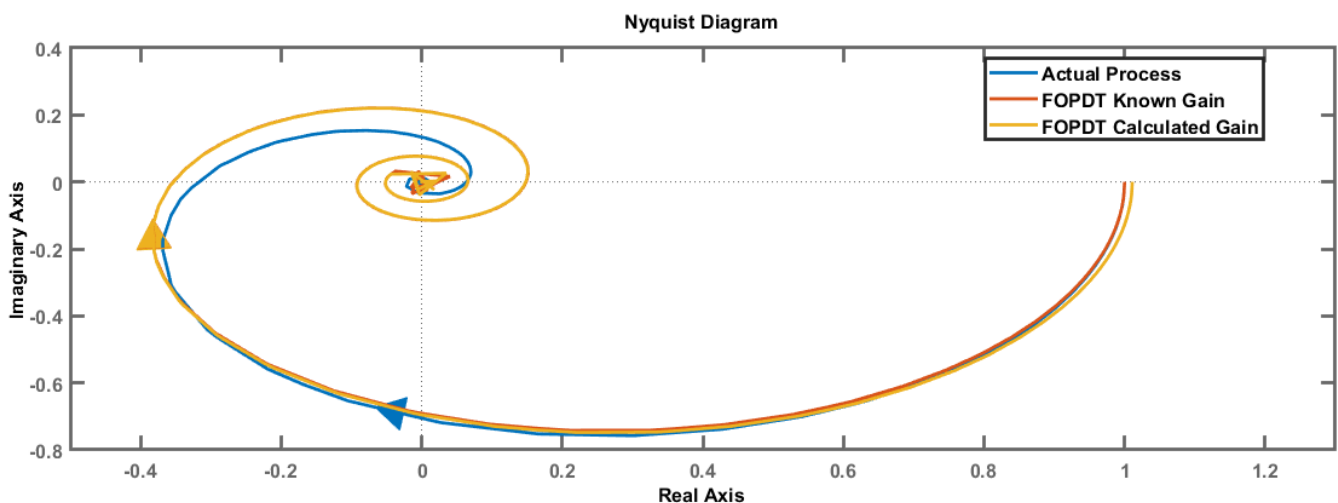


Fig. 6.1: Nyquist Plot of FOPDT for Example 1

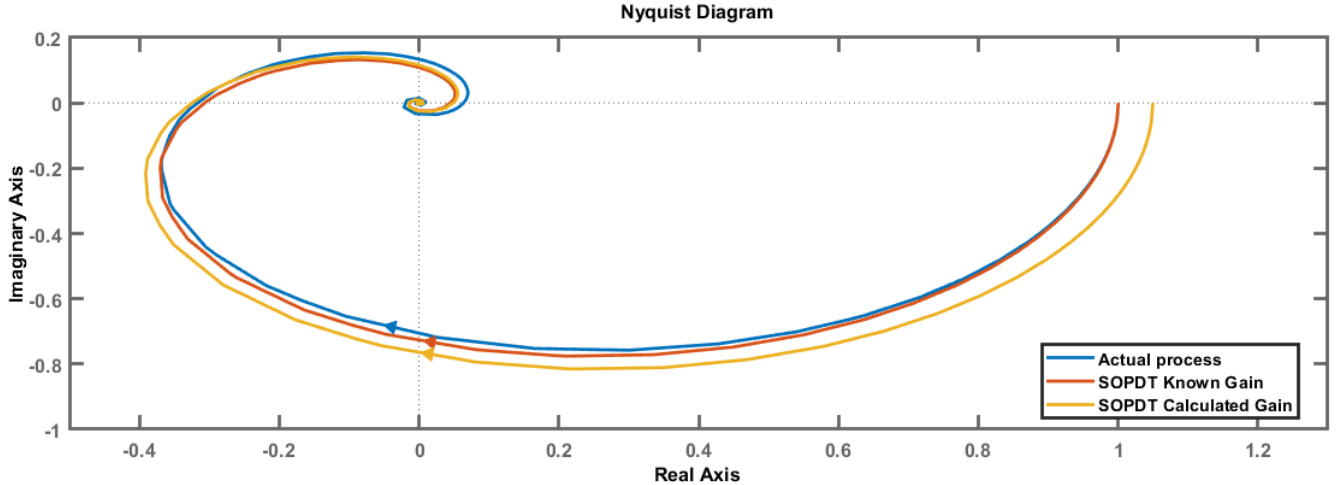


Fig. 6.2: Nyquist Plot of SOPDT for Example 1

Actual Process has been identified using both FOPDT and SOPDT models. The Known Gain and Calculated Gain values are given for both types of models, and the IAE (Integral of Absolute Error) is close to zero for all cases, indicating a good fit between the identified models and the Actual Process.

Furthermore, the Nyquist plots of the Actual Process, FOPDT models (refers to Fig. 6.1), and SOPDT models (refers to Fig. 6.2) are all close to each other. This suggests that the identified models accurately capture the frequency response and dynamics of the Actual Process.

In terms of the Nyquist plot interpretation, the close proximity of the plots implies that the phase and gain margins of the identified models are in good agreement with the Actual Process. The phase margin indicates the stability margin of the system, and the gain margin provides insight into the system's robustness against disturbances or uncertainties. When the Nyquist plots of the identified models closely align with the Nyquist plot of the Actual Process, it indicates that the stability and robustness characteristics of the models are consistent with the real system.

In conclusion, based on the close alignment of Nyquist plots and the low IAE values, it can be inferred that both the FOPDT and SOPDT models provide accurate representations of the Actual Process. The identified models exhibit similar stability and robustness characteristics, as reflected by their Nyquist plots. These findings suggest that the identified models can be used effectively for further analysis, control design, or simulation studies related to the Actual Process.

6.1.2 Controller design

Fractional filter and integer order filter IMC PID controllers are designed for all four process models. The tuning parameter γ , which represents the filter time constant, is selected based on the margin of the identified process model, specifically the period ' T_u ' at which the process becomes marginally stable. In all models, γ is chosen to be 10 per cent of T_u , as specified in Table 6.2.

Table 6.2: Comparison of filters Example 1

	Integer order	Fractional order
Filter FOPDT known gain	$f_1 = \frac{7.397s + 1}{35.579s + 19.604}$	$f_1 = \frac{(7.397s + 1)}{35.579s^{1.1} + 4.8099s^{0.1} + 14.794}$
Controller FOPDT known gain		$G_c = \frac{20.229}{0.3} \left(1 + \frac{1}{20.229s}\right)$
Filter FOPDT calculated gain	$f_1 = \frac{7.378s + 1}{35.475s + 19.564}$	$f_1 = \frac{(7.378s + 1)}{35.475s^{1.1} + 4.8082s^{0.1} + 14.756}$
Controller FOPDT calculated gain		$G_c = \frac{20.2661}{0.3} \left(1 + \frac{1}{20.4870s}\right)$
Filter SOPDT known gain	$f_1 = \frac{4.5283s + 1}{21.91s + 13.895}$	$f_1 = \frac{(4.5283s + 1)}{21.91s^{1.1} + 4.8383s^{0.1} + 9.0567}$
Controller SOPDT known gain		$G_c = \frac{23.0980}{0.3} \left(1 + \frac{1}{23.0980s} + 5.7745s\right)$
Filter SOPDT calculated gain	$f_1 = \frac{4.5078s + 1}{21.603s + 13.808}$	$f_1 = \frac{4.5078s + 1}{21.603s^{1.1} + 4.7924s^{0.1} + 9.0156}$
Controller SOPDT calculated gain		$G_c = \frac{21.6617}{0.3} \left(1 + \frac{1}{22.7340s} + 5.6835s\right)$
Controller Method in [17] SOPDT model		$G_C(s) = \frac{2.3}{0.3} \left(1 + \frac{1}{23s} + 4.4347s\right)$

Table 6.3: Comparison of IAE, ISE and TV Example 1

		Integer order				Fractional order			
	Tu	p	IAE	ISE	TV	P	IAE	ISE	TV
FOPDT Known Gain	4.809	1	22.4421	16.5697	26.8894	1.1	21.9127	16.4252	20.9559
FOPDT Calculated Gain	4.808	1	22.4018	16.5298	26.9608	1.1	21.8726	16.3855	21.0120
SOPDT Known Gain	4.838	1	14.4627	10.4737	101760	1.1	13.9926	10.3544	5460.8
SOPDT Calculated Gain	4.792	1	14.4554	10.4256	93163	1.1	13.9880	10.3076	5089.4
Method in [17] SOPDT model			14.2137	11.5407	6822.7				

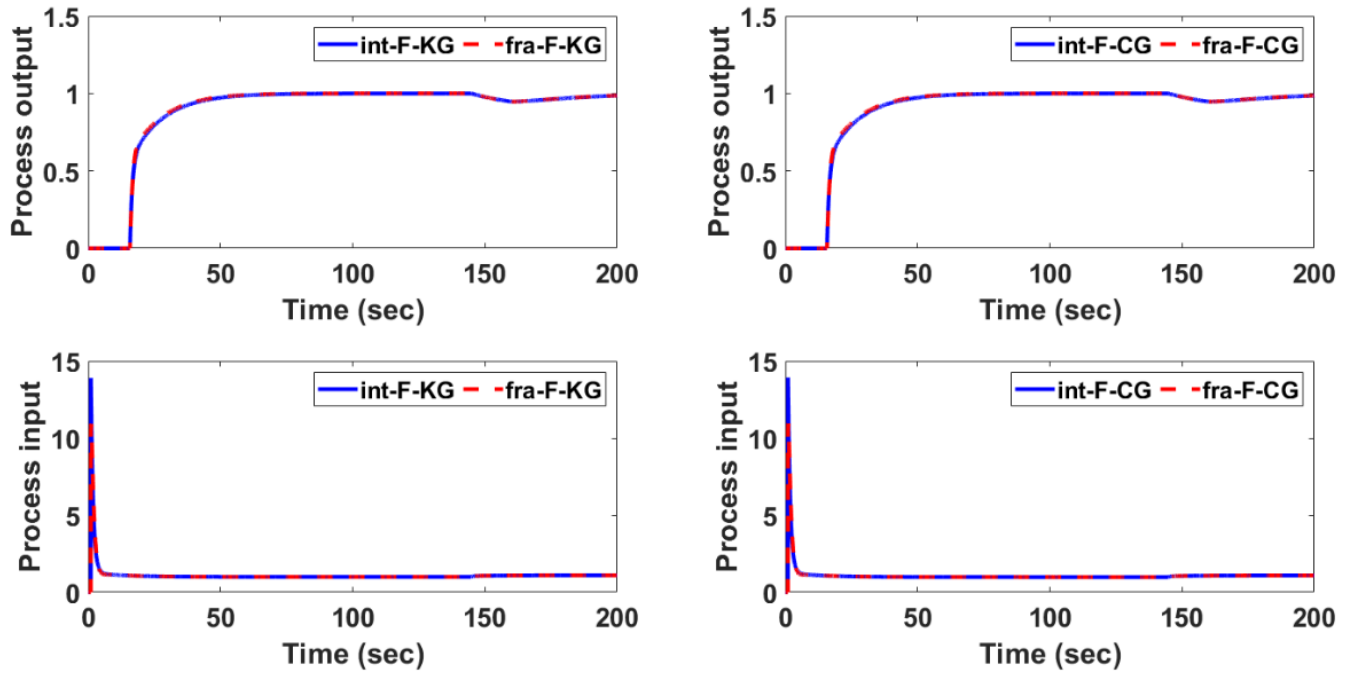


Fig. 6.3: Response for example 1 FOPDT Process

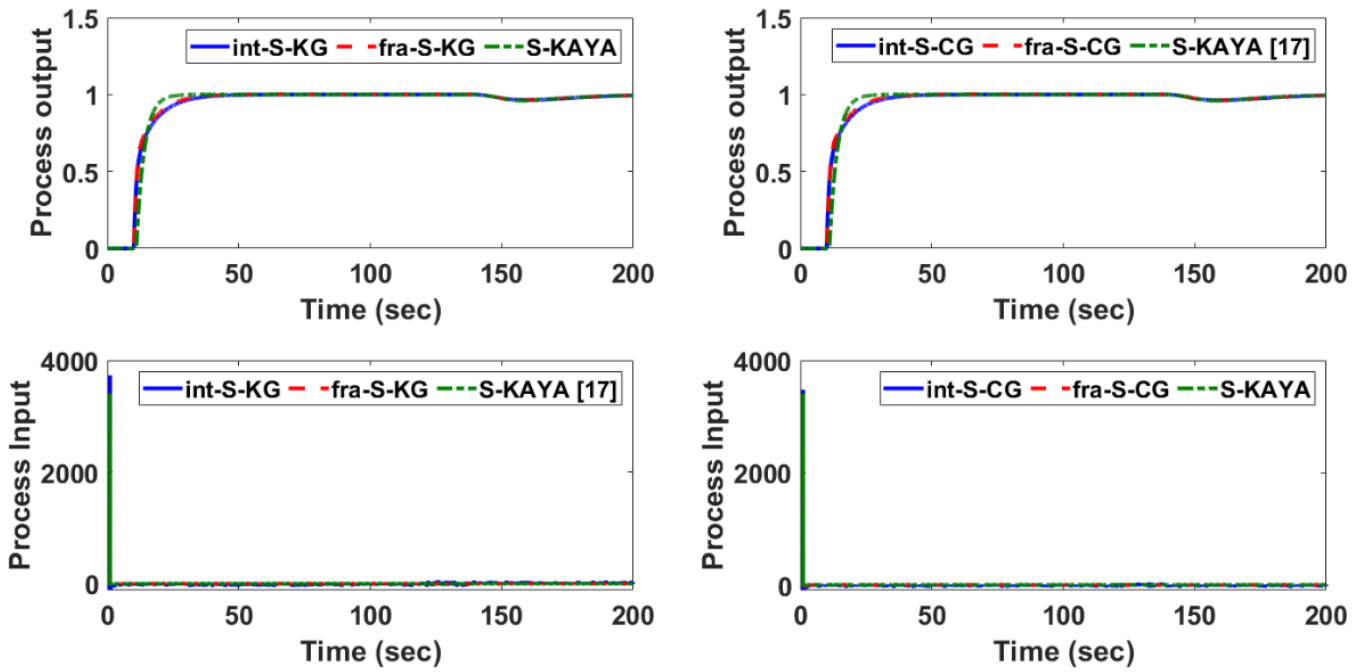


Fig. 6.4: Response for example 1 SOPDT Process

Overall, the fractional-order IMC PID controllers exhibit comparable or slightly better performance than their integer-order counterparts for both FOPDT and SOPDT process models, particularly in terms of the IAE, ISE, and TV indices. The calculated gain tends to deliver slightly improved results compared to the known gain in terms of the performance indices IAE and ISE for both the FOPDT and SOPDT models. Furthermore, the fractional-order controller consistently outperforms a specific method presented in [17] for the SOPDT model, especially regarding the IAE, ISE, and TV indices, demonstrating its superiority in terms of overall performance (refers table 6.3, Fig.6.3 & Fig. 6.4).

6.1.3 Robust Analysis

Table 6.4: Performance Criteria for Perturbations in Process Model (Example 1)

Controller		+10% perturbation		-10% perturbation		+20% perturbation		-20% perturbation	
		IAE	TV	IAE	TV	IAE	TV	IAE	TV
FOPDT Known Gain	Integer	23.4088	54.8805	22.5610	55.0544	28.5971	104.3014	25.3892	108.1414
	Fractional	23.3576	56.2143	22.2346	56.1997	31.2747	154.0297	29.2767	169.1730
FOPDT Calculated Gain	Integer	23.3621	54.9172	22.5181	55.1548	28.5412	104.4095	25.3210	108.1763
	Fractional	23.3088	56.1465	22.1892	56.2066	31.1975	153.9163	29.1657	169.1203
SOPDT Known Gain	Integer	14.6351	104010	14.4559	103430	16.7068	102480	14.6835	103750
	Fractional	14.4631	5716.3	13.9523	5716.2	17.1400	5980.3	14.6342	5976.5
SOPDT Calculated Gain	Integer	14.6307	95051	14.4485	96444	16.7054	97029	14.6846	96836
	Fractional	14.4592	5330.6	13.9479	5330.5	17.1422	5582.4	14.6497	5578.2
SOPDT-Method in I KAYA[17]		16.1858	6865.2	14.2109	6865.0	18.8751	6888.0	14.6151	6887.1

Based on the analysis of the Table 6.4, the following observations can be made:

For +10% and -10% perturbations:

- Both the FOPDT Known and Calculated Fractional controllers have lower values in terms of IAE compared to other controllers, indicating better performance in terms of error reduction.

For +20% and -20% perturbations:

- The FOPDT Integer controller has better values in terms of IAE and TV compared to other controllers, indicating superior performance in dealing with larger perturbations.

Comparing SOPDT controllers and the literature [17] process:

- The Fractional controllers (both known and calculated) outperform other controllers, including the literature [17] process, in terms of IAE, TV.

In summary, based on the available information in the table, for +10% and -10% perturbations, both FOPDT Known and Calculated Fractional controllers show better performance in terms of IAE. For +20% and -20% perturbations, the FOPDT Integer controller performs better in terms of IAE and TV. When comparing SOPDT controllers and the literature [17] process, the Fractional controllers perform well in terms of IAE, TV. Overall, the fractional controller provides better error reduction and improved control signal stability, particularly for the SOPDT process.

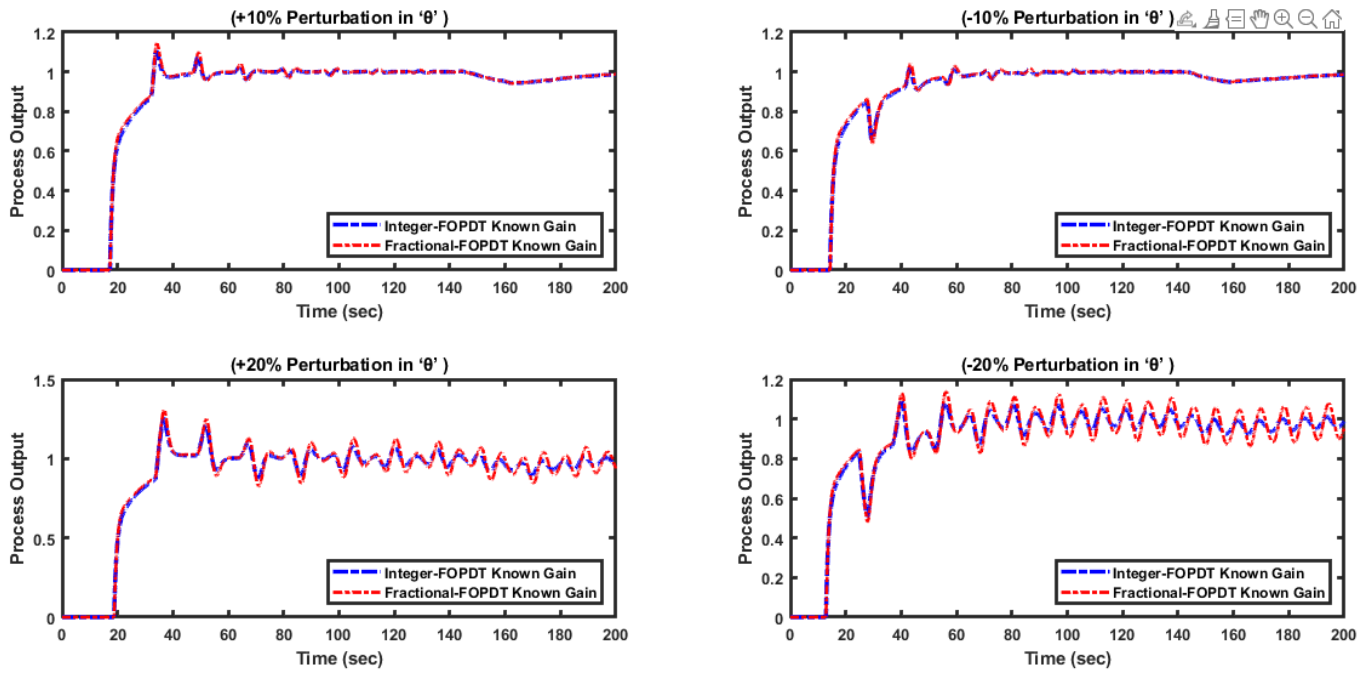


Fig. 6.5: Response of ex.1 for $\pm 10\%$, $\pm 20\%$ change in Time Delay for FOPDT Known Gain

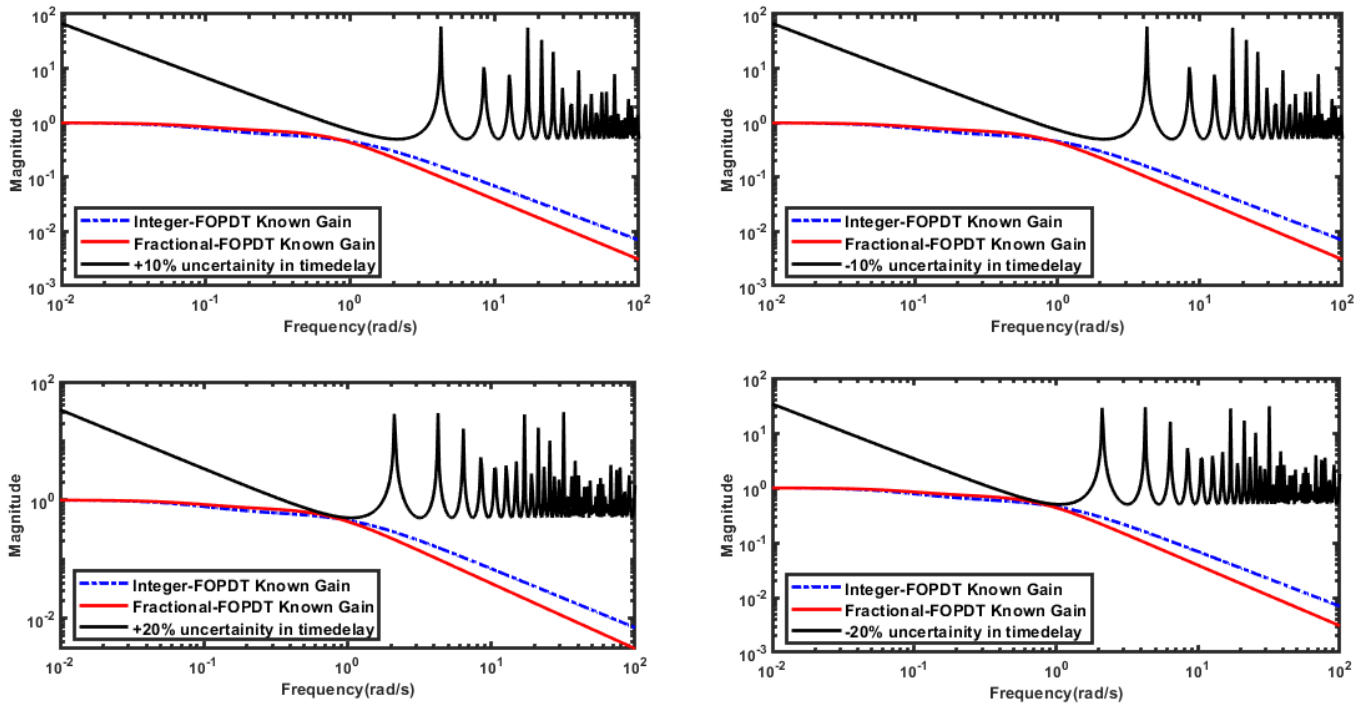


Fig. 6.6: Norm-bound uncertainty of Example 1 for FOPDT Known Gain

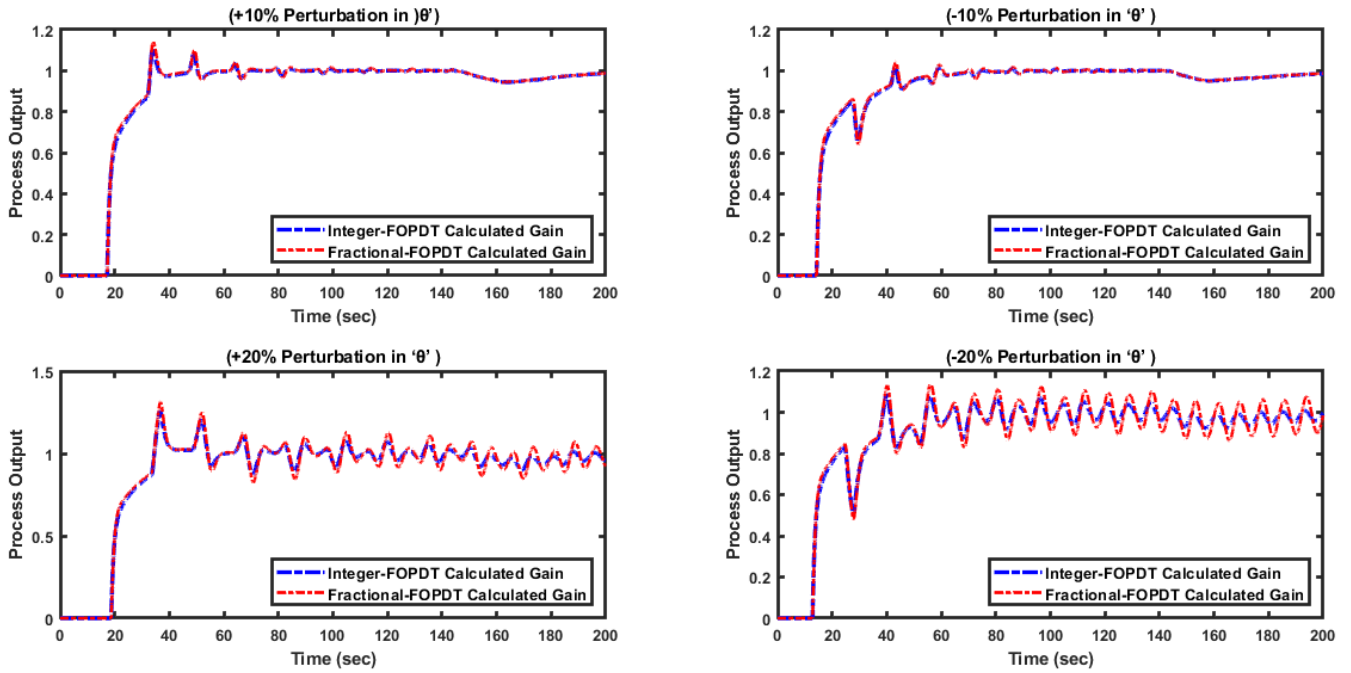


Fig. 6.7: Response of ex.1 for $\pm 10\%$, $\pm 20\%$ change in Time Delay for FOPDT Calculated Gain

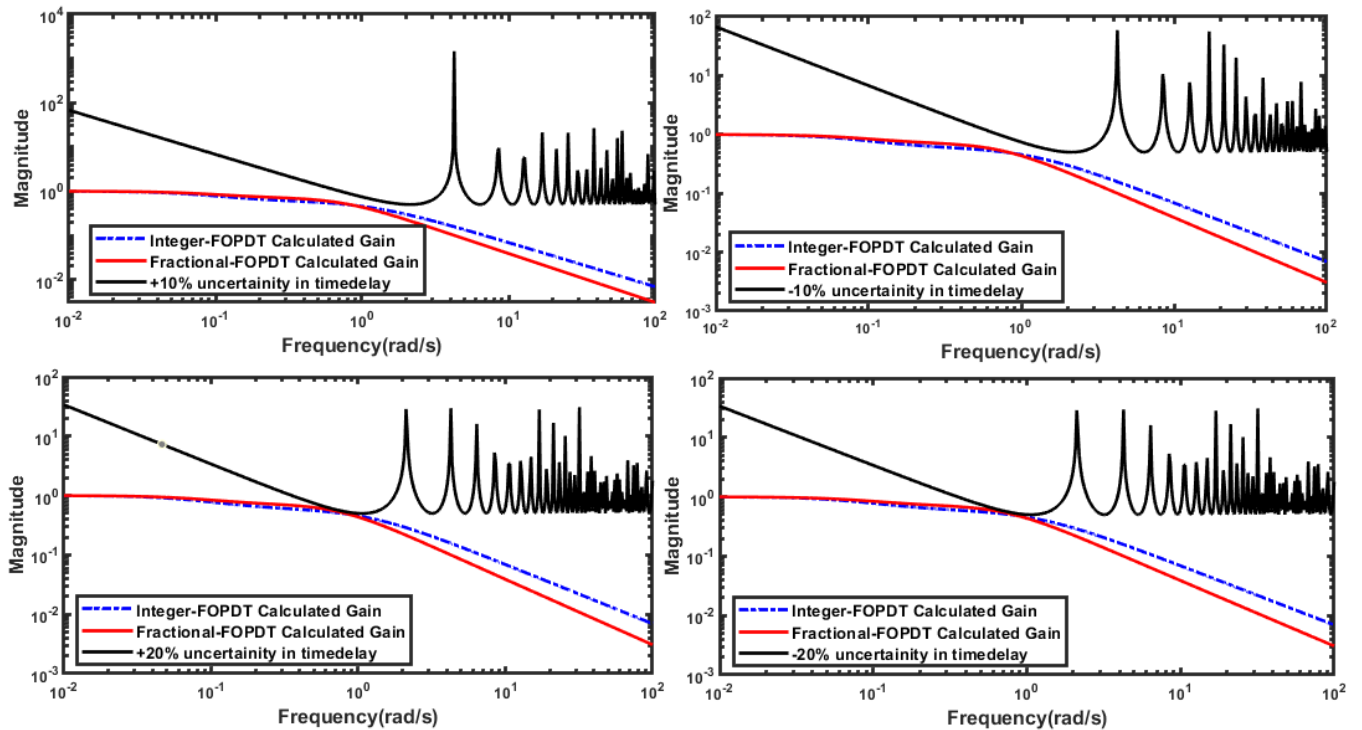


Fig. 6.8: Norm-bound uncertainty of Example 1 for FOPDT Calculated Gain

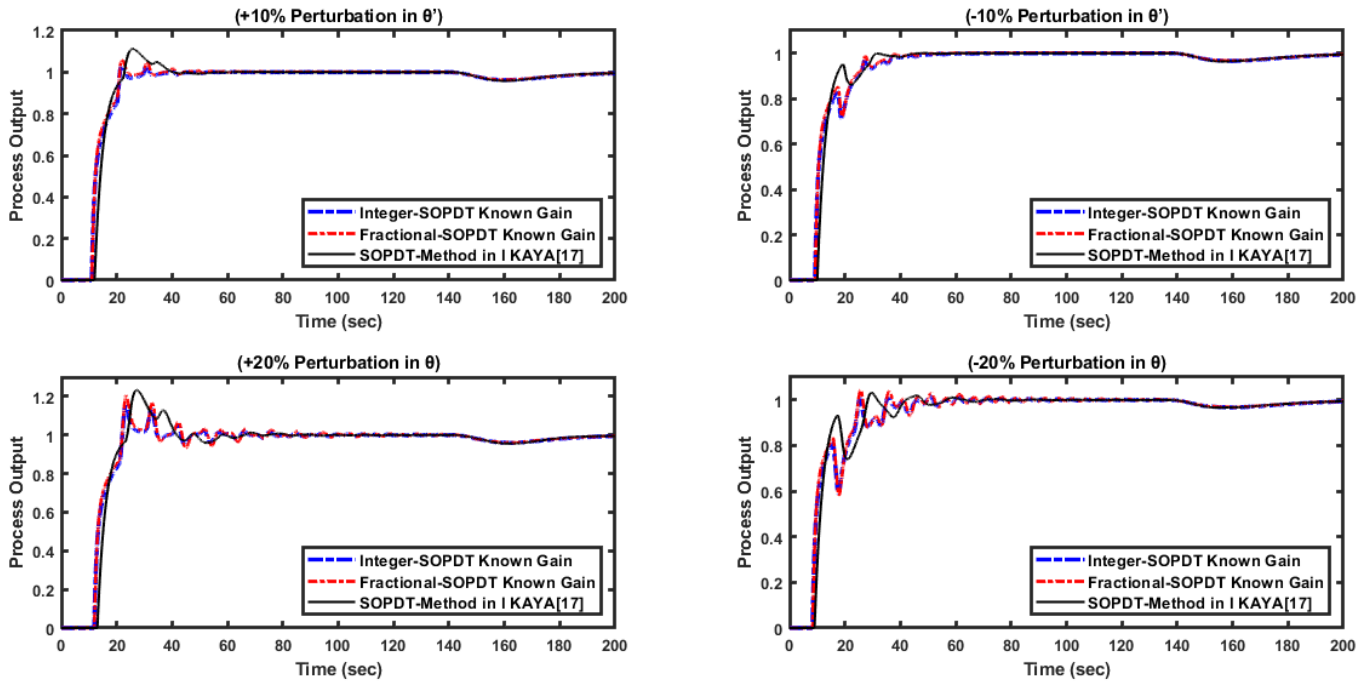


Fig. 6.9: Response of ex.1 for $\pm 10\%$, $\pm 20\%$ change in Time Delay for SOPDT Known Gain

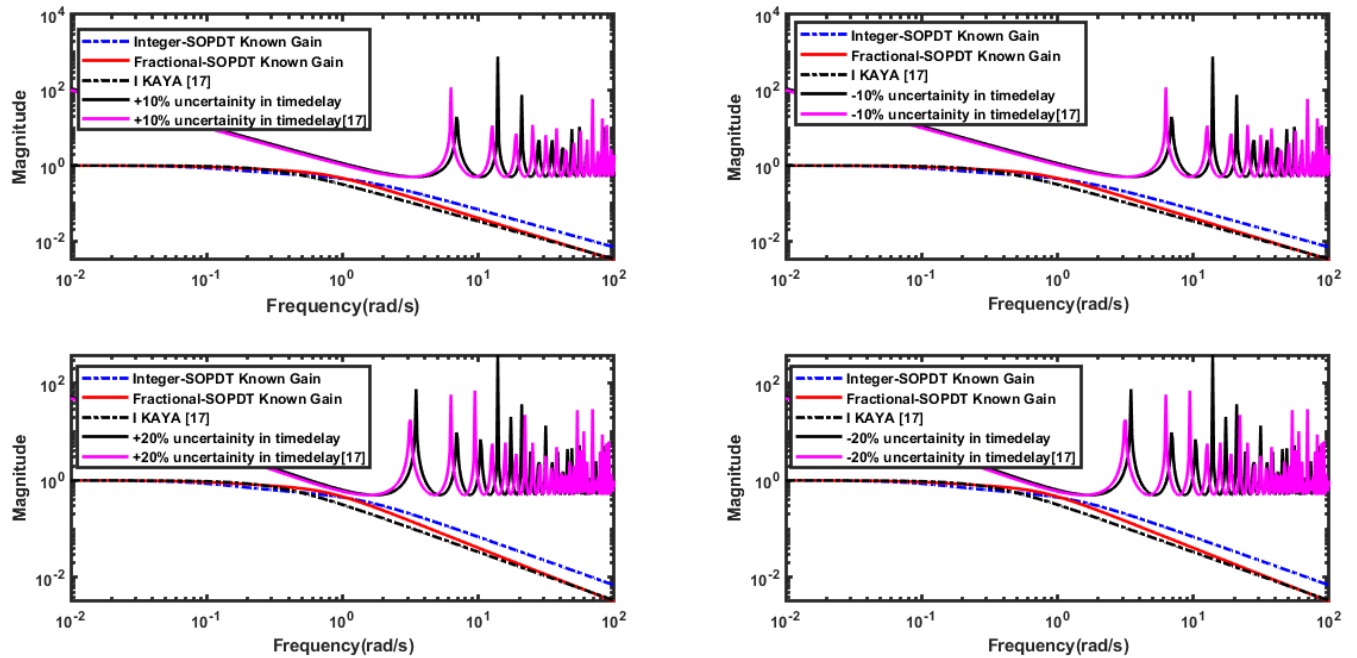


Fig. 6.10: Norm-bound uncertainty of Example 1 for SOPDT Known Gain

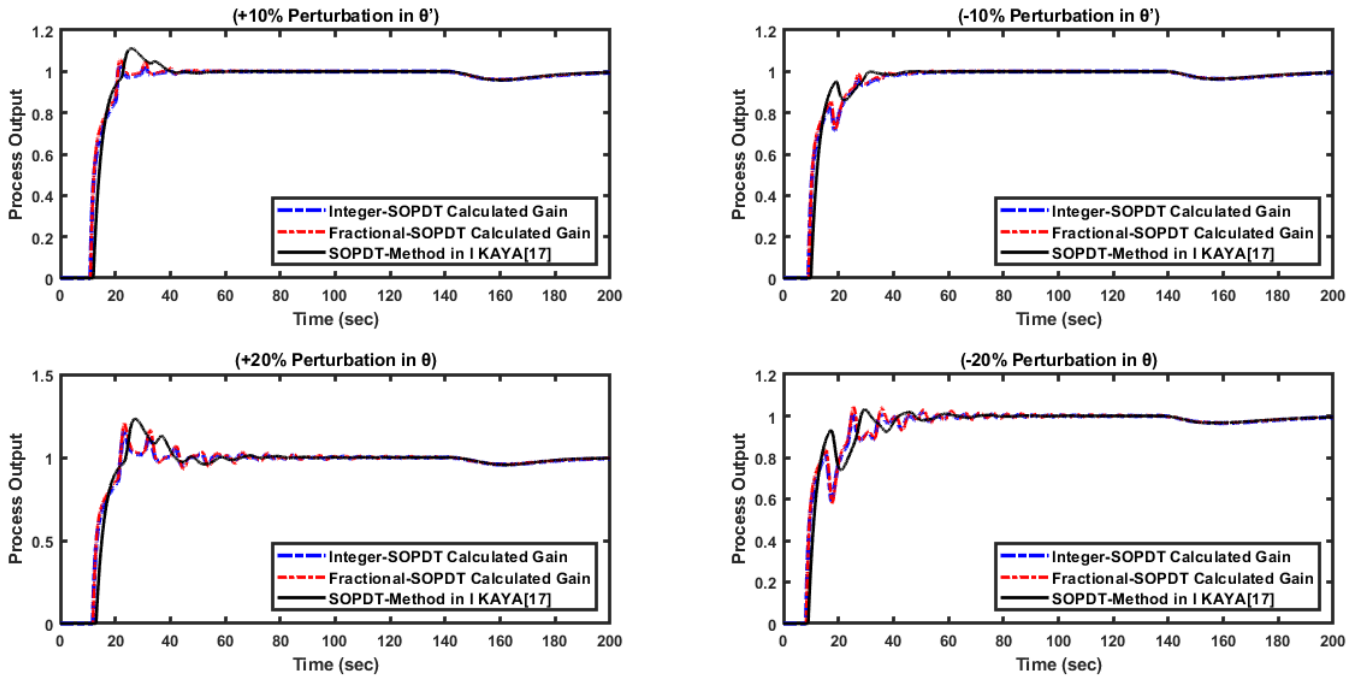


Fig. 6.11: Response of ex.1 for $\pm 10\%$, $\pm 20\%$ change in Time Delay for SOPDT Calculated Gain

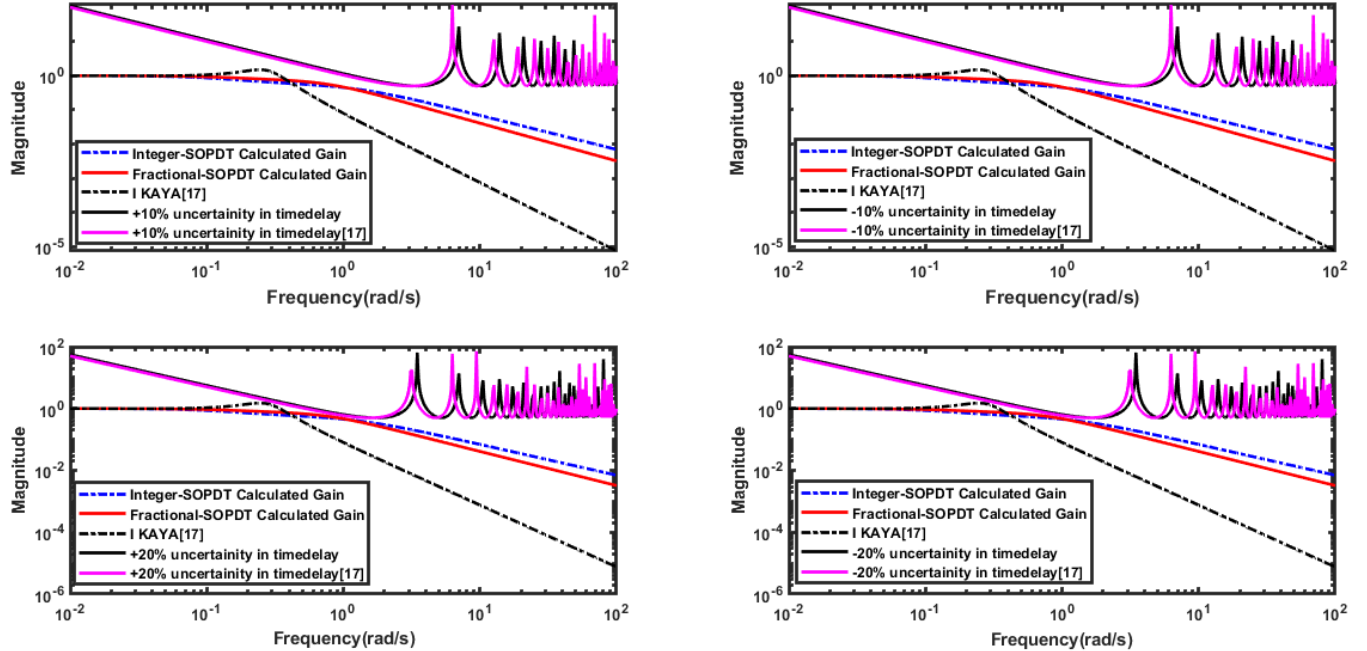


Fig. 6.12: Norm-bound uncertainty of Example 1 for SOPDT Calculated Gain

6.2 Example 2

$$G_2(s) = \frac{e^{-10s}}{(s+1)^2}$$

6.2.1 Identification

A relay with parameters $h_1=1.5$, $h_2=-1$, $\varepsilon=\pm 0.025$ and $\alpha=0.1$ to 1.8 is applied to the system mentioned above to generate a limit cycle. The chosen data is based on minimizing the IAE and ISE. The measured limit cycle information for all four models at $\alpha=0.1$ is $A_P = 1.4997$, $A_V = 0.9999$, and $T = 24.4767$. The identified process models (refers to Table 6.5) are compared with actual models and methods described in the literature, focusing on IAE and Nyquist plots.

Table 6.5: Comparison of proposed models Example 2

α	METHODS	MODEL	IAE
	Actual process	$\frac{e^{-10s}}{(s+1)^2}$	--
0.1	FOPDT Known gain	$\frac{e^{-9.049s}}{(2.906s+1)}$	0.0194
0.1	FOPDT Calculated gain	$\frac{0.9920 e^{-9.092s}}{(2.841s+1)}$	0.0280
0.1	SOPDT Known gain	$\frac{e^{-7.948s}}{(1.938s+1)^2}$	0.0195
0.1	SOPDT Calculated gain	$\frac{0.9920 e^{-8.012s}}{(1.899s+1)^2}$	0.0280
	Method in [17] FOPDT model	$\frac{e^{-10.87s}}{(1.27s+1)}$	0.0485
	Method in [17] SOPDT model	$\frac{e^{-10s}}{(s+1)^2}$	0.000

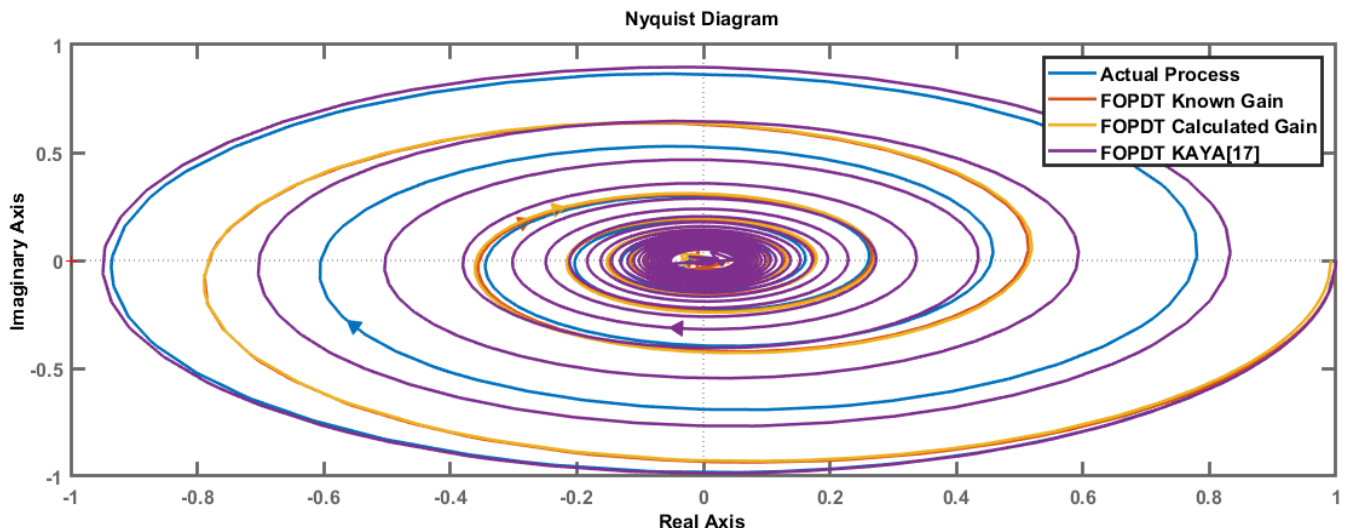


Fig. 6.13: Nyquist Plot of FOPDT for Example 2

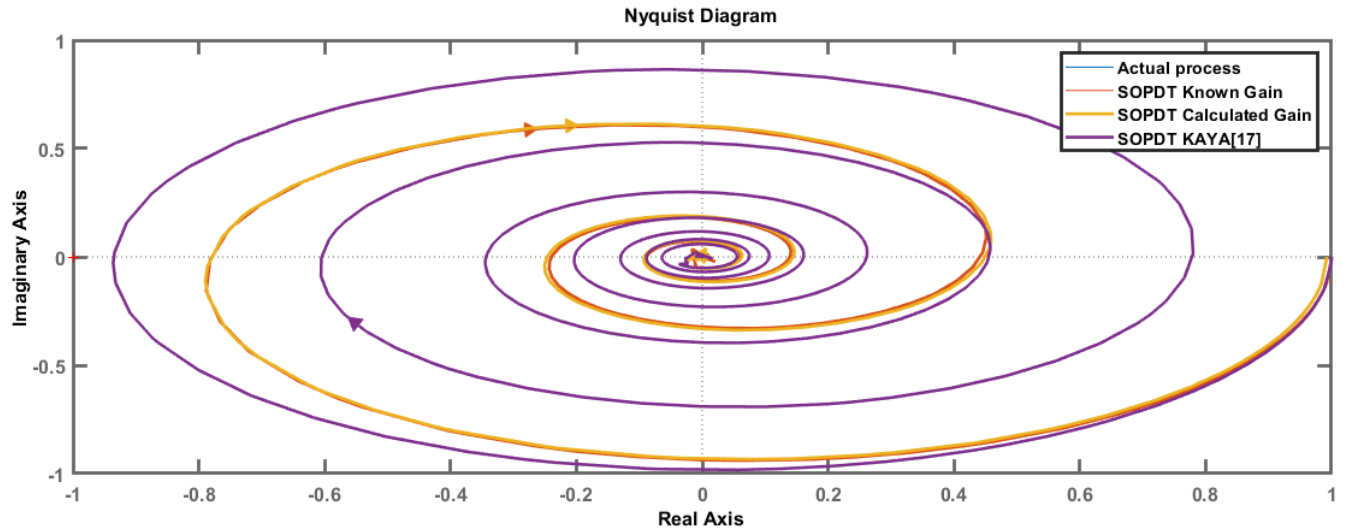


Fig. 6.14: Nyquist Plot of SOPDT for Example 2

The Actual Process has been identified using FOPDT and SOPDT models, and their corresponding Known Gain and Calculated Gain Models are provided in the Table 6.5. The IAE for both models is close to zero, indicating a good fit between the identified models and the Actual Process.

Furthermore, the Nyquist plot (refers to Fig. 6.13) of the Actual Process, FOPDT models (as described in reference [17]), and the identified FOPDT models are all in close proximity to each other. This suggests that the identified models accurately capture the frequency response and dynamics of the Actual Process, as well as align with the FOPDT model described in the reference paper [17].

The same observation can be made for the Nyquist plots of the Actual Process, SOPDT models (refers to Fig. 6.14) (known gain and calculated gain), and the identified SOPDT model. They all exhibit a close resemblance to each other, indicating a good match in terms of stability and robustness characteristics.

Based on the close alignment of Nyquist plots and the low IAE values, it can be concluded that both the FOPDT and SOPDT models, including the ones described in the reference paper [17], provide accurate representations of the Actual Process. These findings affirm the suitability of the identified models for various applications, such as analysis, control design, or simulation studies related to the Actual Process.

6.2.2 Controller design

IMC PID controllers, both fractional-order and integer-order filters, have been designed for all four process models. The selection of the tuning parameter γ , which represents the filter time constant, is based on the margin observed in the identified process model at the marginally stable period 'Tu'. In Table 6.6, the value of γ is set to 10 per cent of Tu for all models.

Table 6.6: Comparison of filters Example 2

	Integer order	Fractional order
Filter FOPDT known gain	$f_1 = \frac{4.5245s + 1}{10.413s + 11.351}$	$f_1 = \frac{4.5245s + 1}{10.413s^{1.1} + 2.3015s^{0.1} + 9.049}$
Controller FOPDT known gain		$G_c = \frac{2.9060}{0.5} \left(1 + \frac{1}{2.9060s}\right)$
Filter FOPDT calculated gain	$f_1 = \frac{4.546s + 1}{10.463s + 11.394}$	$f_1 = \frac{4.546s + 1}{10.463s^{1.1} + 2.3017s^{0.1} + 9.092}$
Controller FOPDT calculated gain		$G_c = \frac{2.8639}{0.5} \left(1 + \frac{1}{2.8410s}\right)$
Filter SOPDT known gain	$f_1 = \frac{3.974s + 1}{9.1508s + 10.251}$	$f_1 = \frac{3.974s + 1}{9.1508s^{1.1} + 2.3027s^{0.1} + 7.948}$
Controller SOPDT known gain		$G_c = \frac{3.8760}{0.5} \left(1 + \frac{1}{3.8760s} + 0.9690s\right)$
Filter SOPDT calculated gain	$f_1 = \frac{4.006s + 1}{9.2268s + 10.315}$	$f_1 = \frac{4.006s + 1}{9.2268s^{1.1} + 2.3033s^{0.1} + 8.012}$
Controller SOPDT calculated gain		$G_c = \frac{3.8286}{0.5} \left(1 + \frac{1}{3.7980s} + 0.9495s\right)$
Controller Method in [17] FOPDT model		$G_c = \frac{0.1168}{0.5} \left(1 + \frac{1}{1.27s}\right)$
Controller Method in [17] SOPDT model		$G_C = \frac{0.2}{0.5} \left(1 + \frac{1}{2s} + 0.5s\right)$

Table 6.7: Comparison of IAE, ISE and TV Example 2

	Tu	Integer order				Fractional order			
		p	IAE	ISE	TV	P	IAE	ISE	TV
FOPDT Known gain	2.301	1	17.6715	11.2481	4.7629	1.1	17.1844	11.1225	3.6231
FOPDT Calculated gain	2.301	1	17.7254	11.2945	4.6953	1.1	17.2384	11.1688	3.5736
SOPDT Known gain	2.302	1	15.6921	9.9582	1498.4	1.1	15.2206	9.8396	195.8466
SOPDT Calculated gain	2.303	1	15.7866	10.0301	1482.5	1.1	15.3144	9.9111	189.5559

Method in [17] FOPDT model		19.5618	14.1018	1.2000				
Method in [17] SOPDT model		18.0050	12.9688	41.2533				

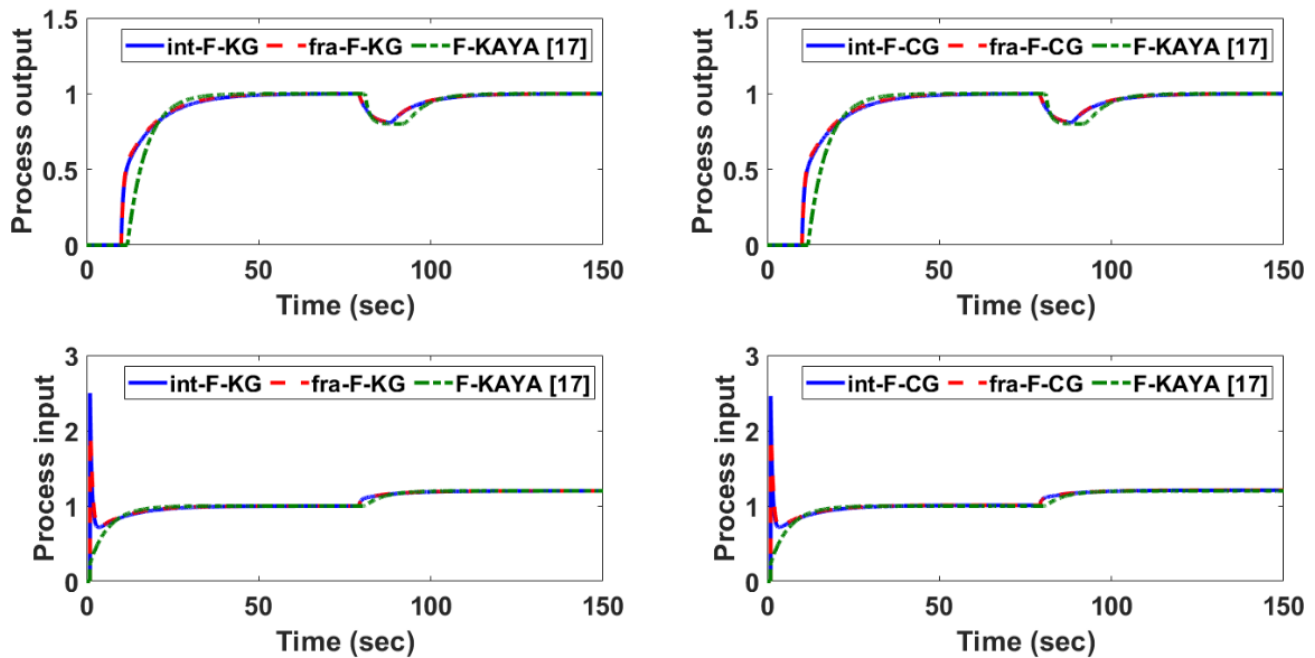


Fig. 6.15: Response of ex.2 FOPDT Process

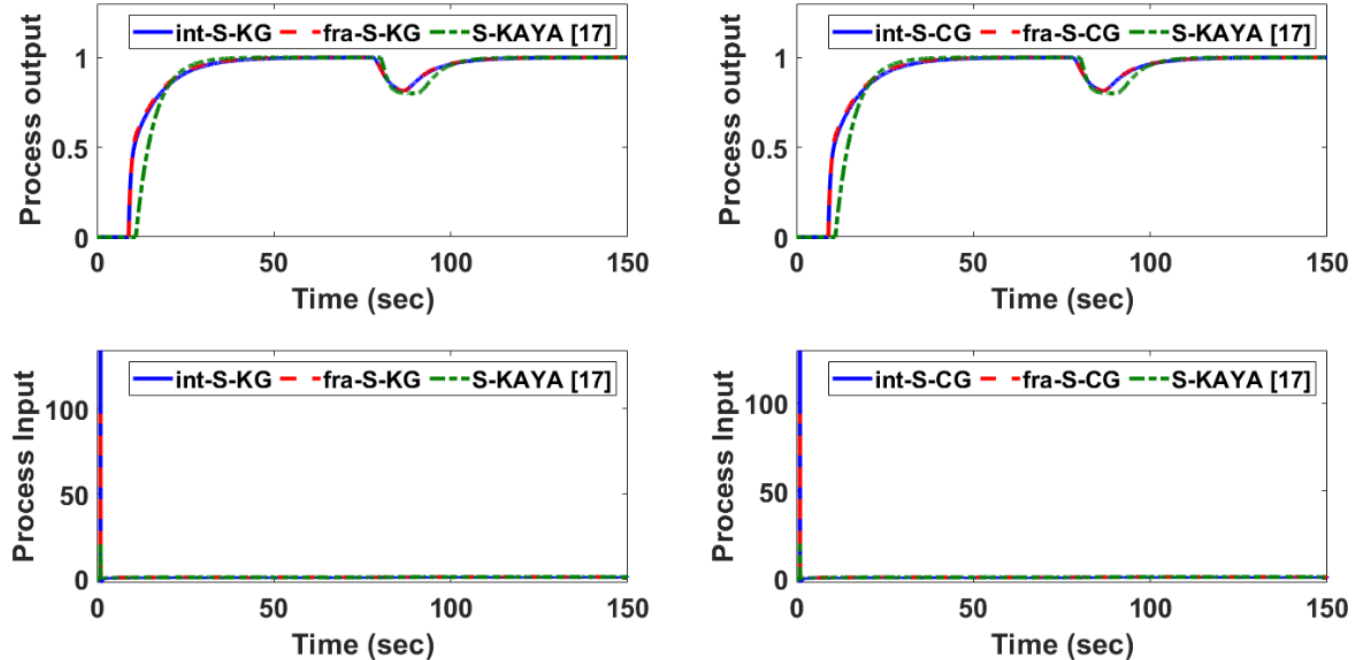


Fig. 6.16 : Response of ex.2 SOPDT Process

In general, the fractional-order IMC PID controllers exhibit similar or slightly superior performance when compared to the integer-order controllers for both the FOPDT and SOPDT process models, especially when evaluating the IAE, ISE, and TV indices. Moreover, when compared to a specific method mentioned in reference [17], the fractional-order controller consistently surpasses it in terms of the IAE and ISE indices, further emphasizing its overall superiority in performance for both the FOPDT and SOPDT models (refers Table 6.7, Fig. 6.15 & Fig.6.16).

6.2.3 Robust Analysis

Table 6.8: Performance Criteria for Perturbations in Process Model (Example 2)

Controller		+10% perturbation		-10% perturbation		+20% perturbation		-20% perturbation	
		IAE	TV	IAE	TV	IAE	TV	IAE	TV
FOPDT Known Gain	Integer	17.6774	7.5095	17.6692	7.4680	18.4269	9.6954	17.6861	9.5102
	Fractional	17.2197	6.6319	17.1149	6.5871	18.4721	10.3804	17.2425	9.8015
FOPDT Calculated Gain	Integer	17.7311	7.4152	17.7229	7.3728	18.4984	9.6599	17.7408	9.3394
	Fractional	17.2737	6.5523	17.1690	6.5116	18.5502	10.3738	17.3014	9.7996
SOPDT Known Gain	Integer	15.6941	1499.2	15.6912	1537.8	16.2431	1528.0	15.6967	1504.1
	Fractional	15.2523	206.269	15.1572	206.296	16.2217	212.238	15.2299	211.649
SOPDT Calculated Gain	Integer	15.7883	1472.7	15.7852	1477.6	16.3523	1455.0	15.7919	1463.0
	Fractional	15.3462	199.688	15.2506	199.717	16.3368	205.706	15.3282	205.123
FOPDT-Method in KAYA[17]		21.0280	1.3143	19.5714	1.2664	23.8633	1.5408	19.5677	1.3795
SOPDT-Method in I KAYA[17]		19.3425	41.4581	18.0042	41.4362	21.9653	41.6965	18.0022	41.5754

Analysing the given Table 6.8, we can draw the following overall conclusions:

IAE Comparison: Among the controllers considered, the SOPDT Calculated Gain Controller (Fractional) consistently performs the best in terms of IAE, exhibiting the lowest IAE values across different perturbations. The FOPDT Known Gain Controller (Fractional) also performs relatively well in terms of IAE. The FOPDT-Method in KAYA [17] and SOPDT-Method in I KAYA [17] controllers generally have higher IAE values compared to the other controllers.

TV Comparison: In terms of TV, the FOPDT Known Gain Controller (Fractional) consistently performs the best, exhibiting the lowest TV values across different perturbations. The SOPDT Calculated Gain Controller (Fractional) also demonstrates good performance in terms of TV.

Controller Comparison: Overall, considering both IAE and TV, the SOPDT Calculated Gain Controller (Fractional) shows relatively better performance compared to the other controllers in terms of minimizing both IAE and TV. The FOPDT Known Gain Controller (Fractional) performs well in terms of TV but slightly worse than the SOPDT Calculated Gain Controller in terms of IAE. The

FOPDT-Method in KAYA [17] and SOPDT-Method in KAYA [17] controllers generally have higher IAE values compared to the other controllers.

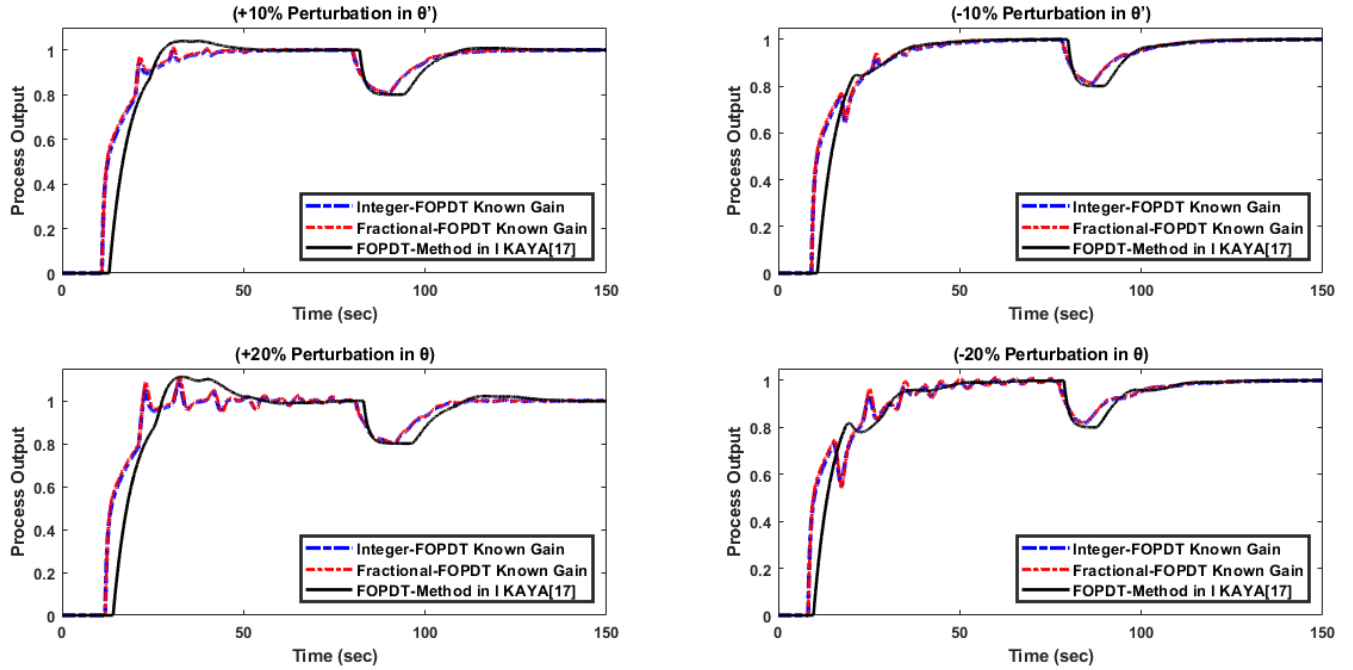


Fig. 6.17: Response of ex.2 for $\pm 10\%$, $\pm 20\%$ change in Time Delay for FOPDT Known Gain

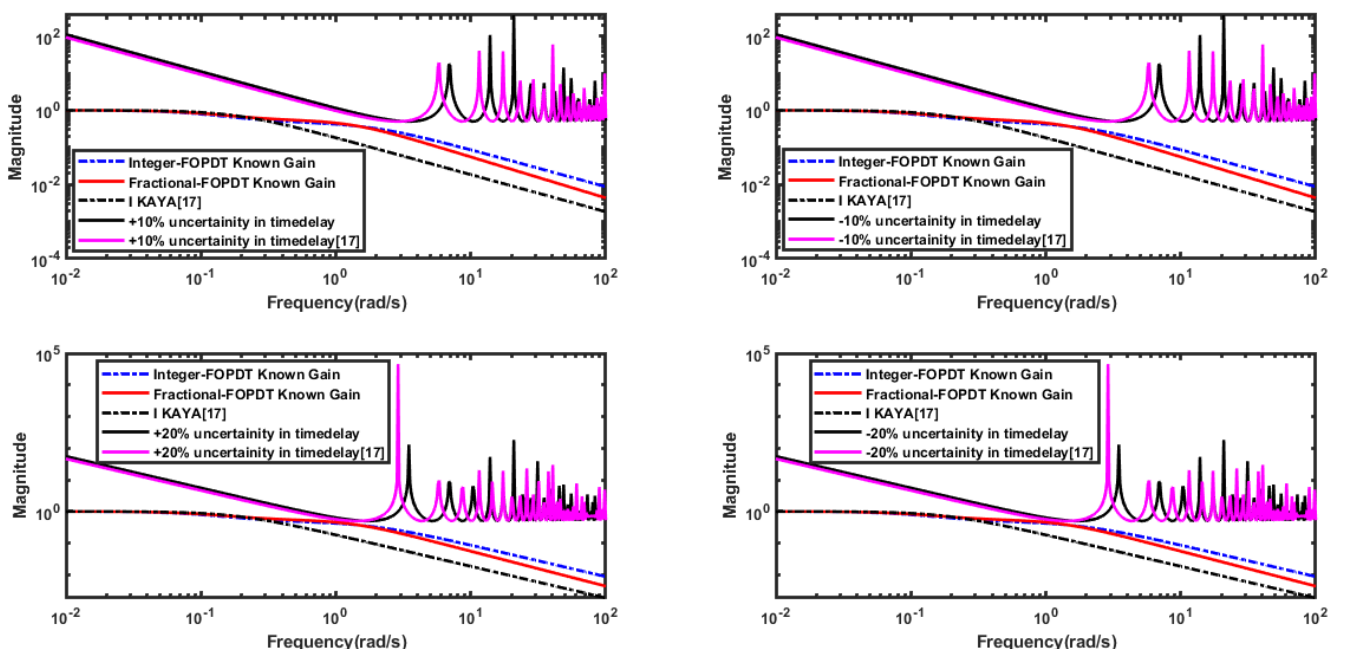


Fig. 6.18: Norm-bound uncertainty of Example 2 for FOPDT Known Gain

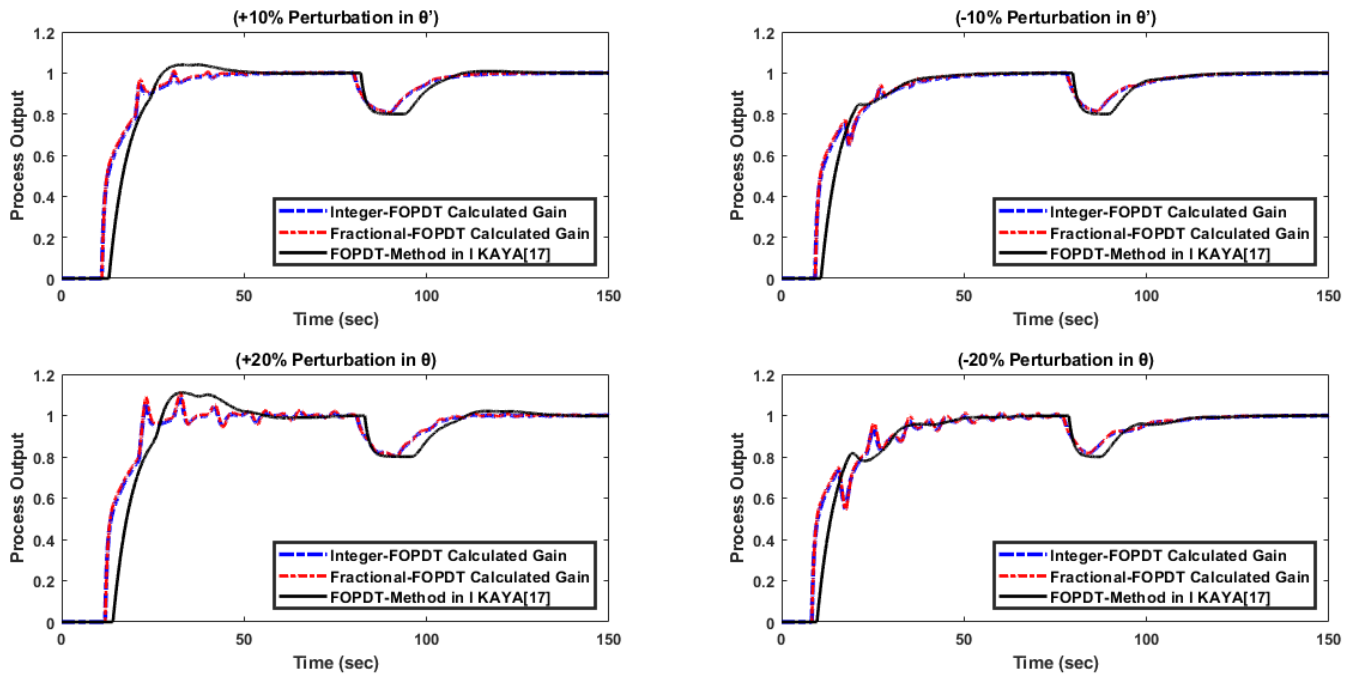


Fig. 6.19: Response of ex.2 for $\pm 10\%$, $\pm 20\%$ change in Time Delay for FOPDT Calculated Gain

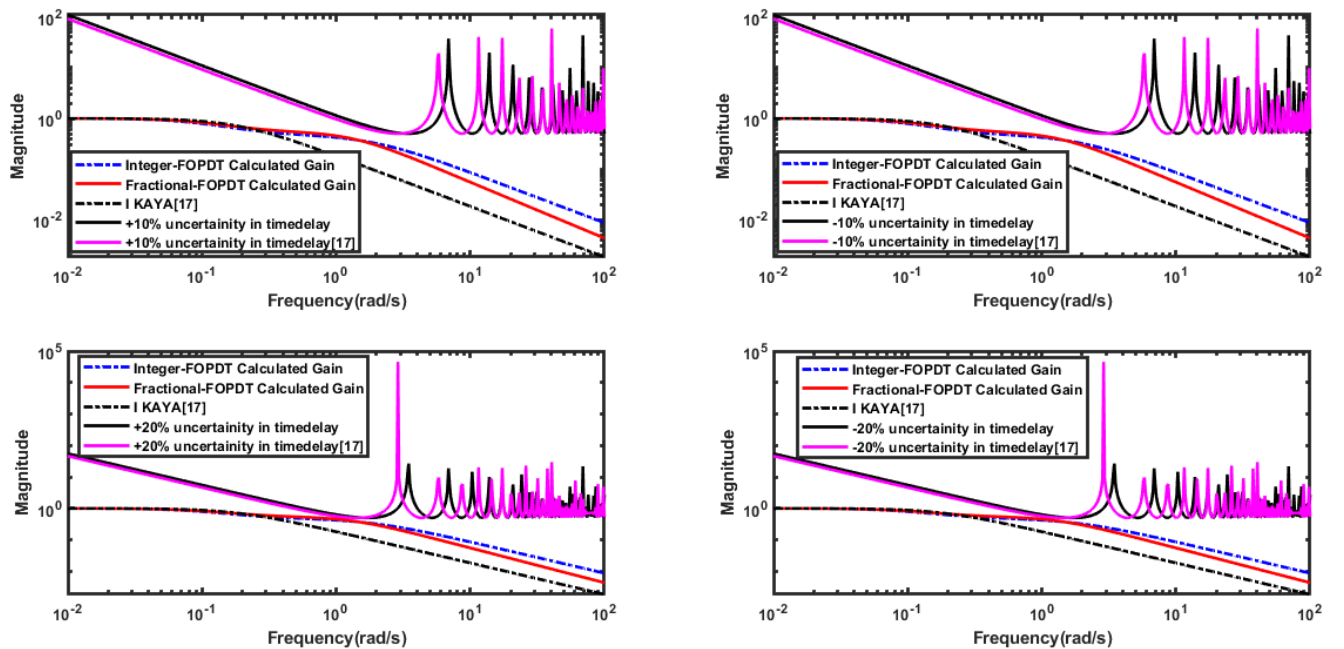


Fig. 6.20: Norm-bound uncertainty of Example 2 for FOPDT Calculated Gain

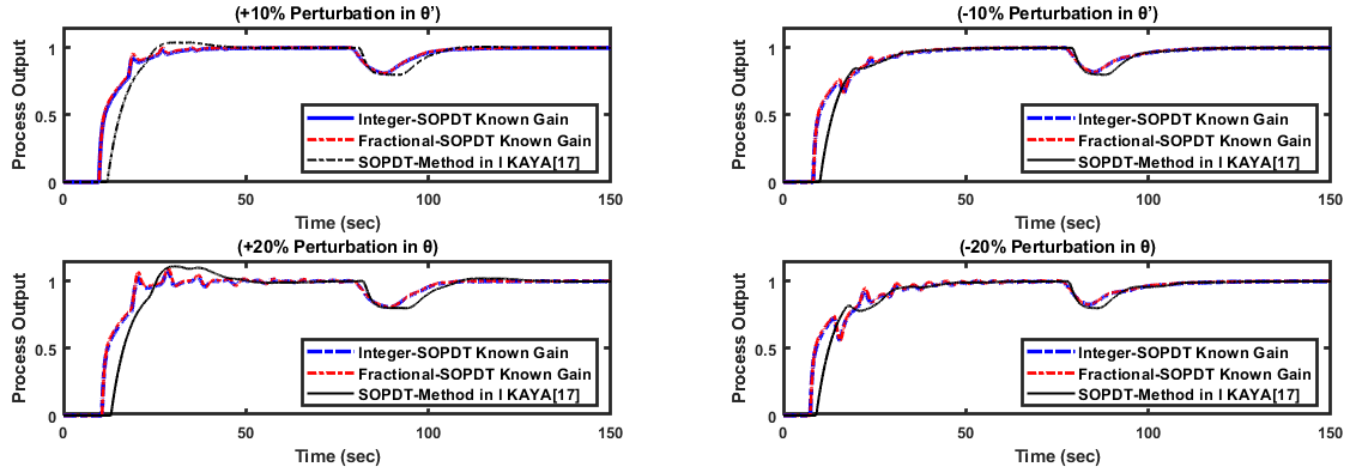


Fig. 6.21: Response of ex.2 for $\pm 10\%$, $\pm 20\%$ change in Time Delay for SOPDT Known Gain

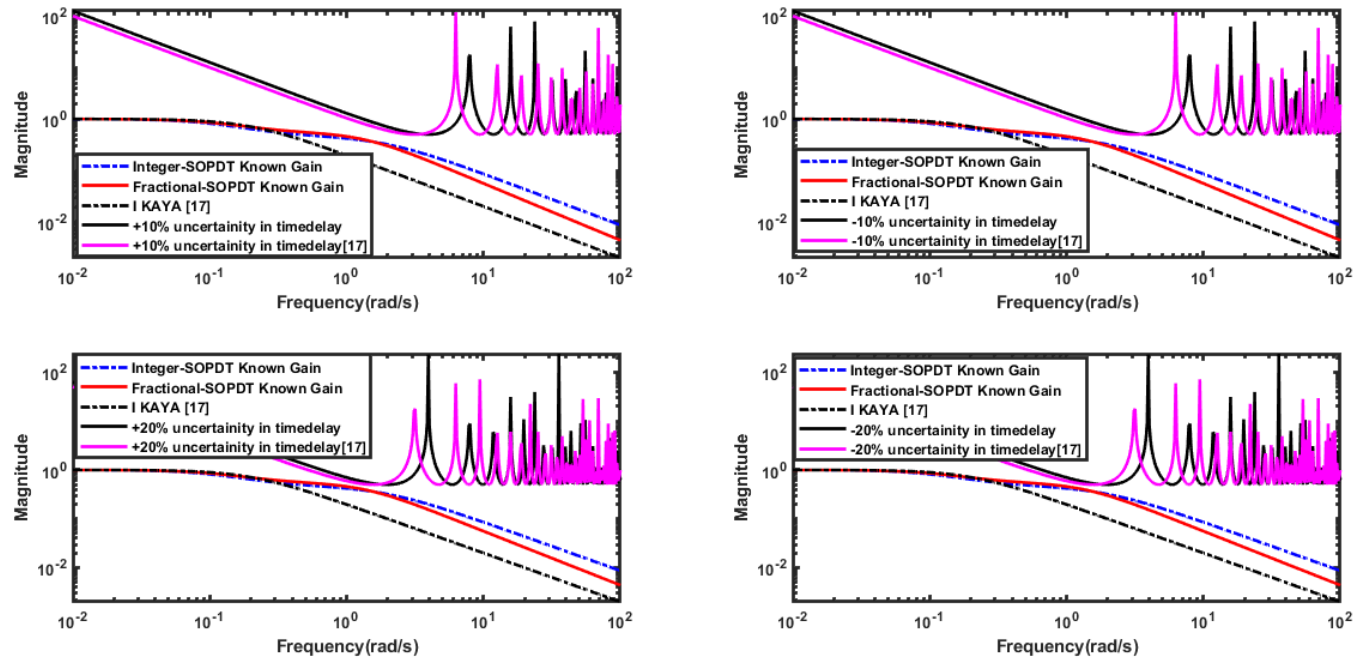


Fig. 6.22: Norm-bound uncertainty of Example 2 for SOPDT Known Gain

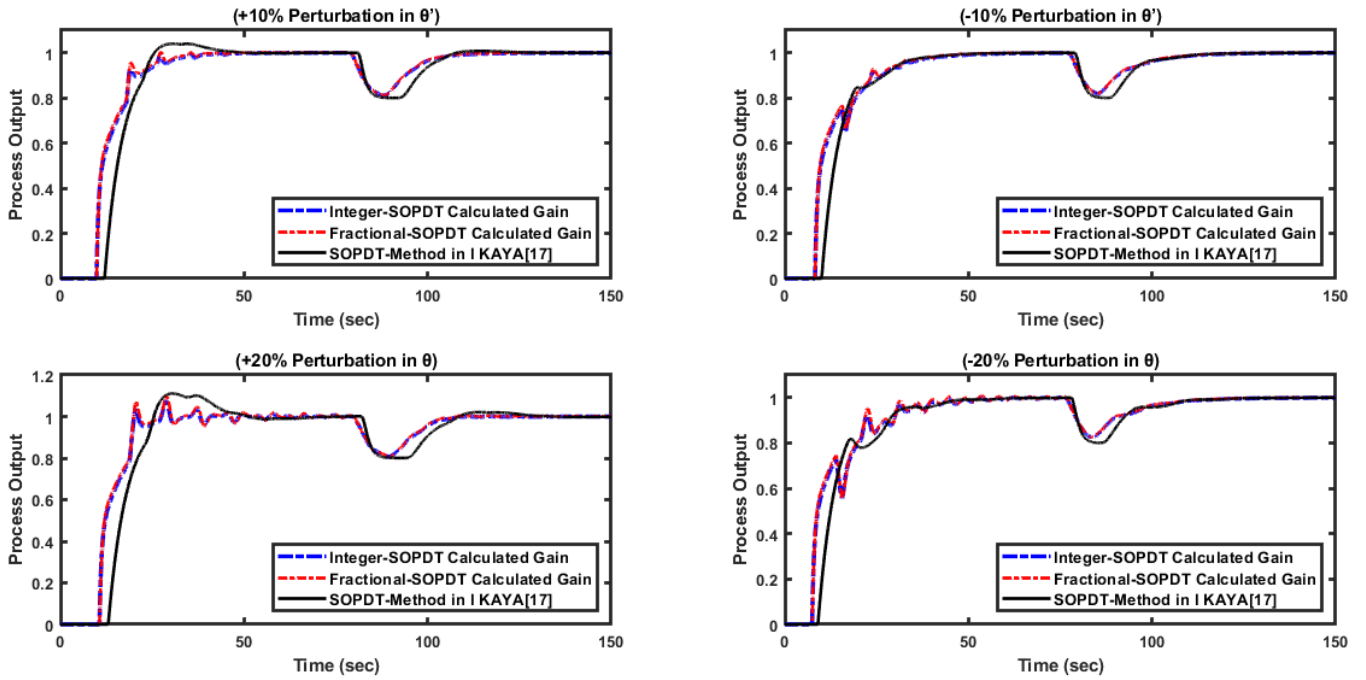


Fig. 6.23: Response of ex.2 for $\pm 10\%$, $\pm 20\%$ change in Time Delay for SOPDT Calculated Gain

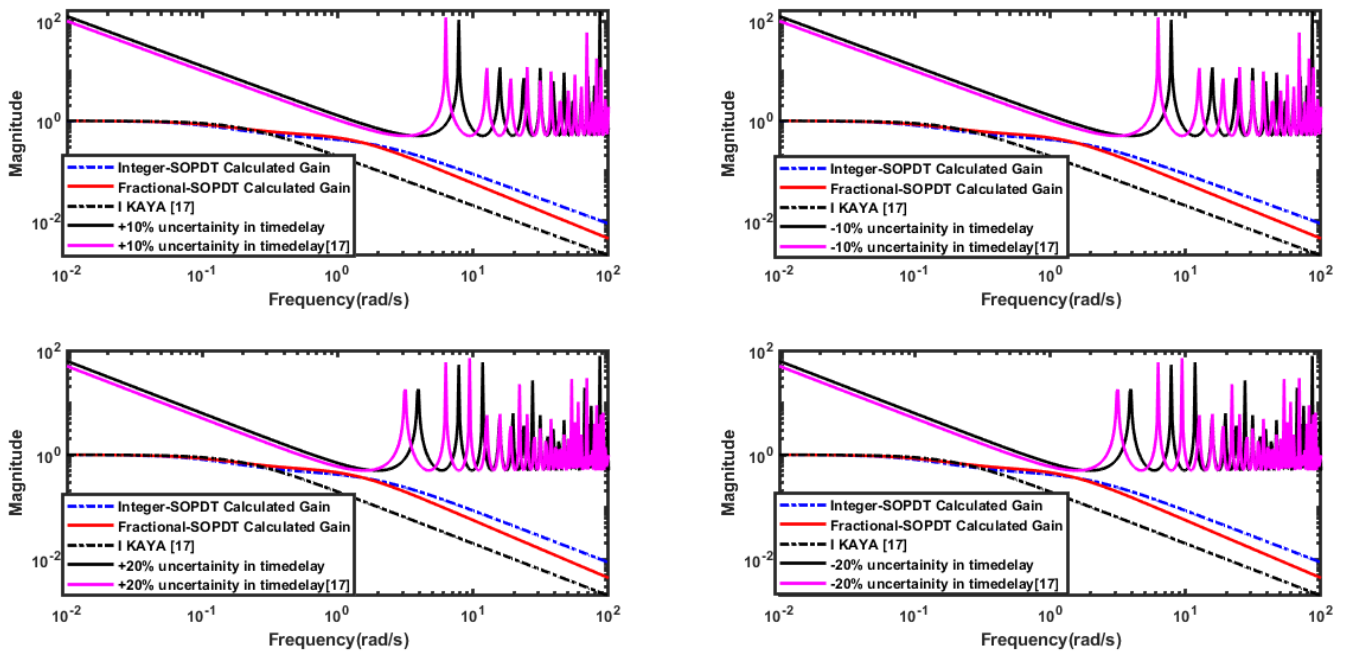


Fig. 6.24: Norm-bound uncertainty of Example 2 for SOPDT Calculated Gain

6.3 Example 3

$$G_3(s) = \frac{e^{-20s}}{(3s + 1)(2s + 1)(s + 1)(0.5s + 1)}$$

6.3.1 Identification

A relay with the specified parameters, including $h_1=1.5$, $h_2=-1$, $\varepsilon=\pm 0.025$, and α ranging from 0.1 to 1.8, is utilized to induce a limit cycle in the system mentioned above. To identify the models with the minimum IAE values, the appropriate α , T , k , τ , and θ values are determined. For all four models, the measured limit cycle information corresponds to $\alpha=0.1$, $T=54.03$, $A_P=1.4975$, and $A_V=0.9989$. By comparing the identified process models (refers to Table 6.9) with the actual system and methods described in the literature, particularly focusing on the IAE and Nyquist plots.

Table 6.9: Comparison of proposed models Example 3

α	METHODS	MODEL	IAE
	Actual process	$\frac{e^{-20s}}{(3s + 1)(2s + 1)(s + 1)(0.5s + 1)}$	--
	Method in [17] FOPDT model	$\frac{e^{-23.28s}}{(3.67s + 1)}$	0.0030
	Method in [17] SOPDT model	$\frac{e^{-21.01s}}{(2.77s + 1)^2}$	0.00039
0.1	FOPDT Known gain	$\frac{e^{-19.963s}}{(6.441s + 1)}$	0.0075
0.1	FOPDT Calculated gain	$\frac{1.0063 e^{-19.892s}}{(6.552 s + 1)}$	0.0073
0.1	SOPDT Known gain	$\frac{e^{-17.525s}}{(4.294s + 1)^2}$	0.0077
0.1	SOPDT Calculated gain	$\frac{1.0063 e^{-17.418s}}{(4.361s + 1)^2}$	0.0074

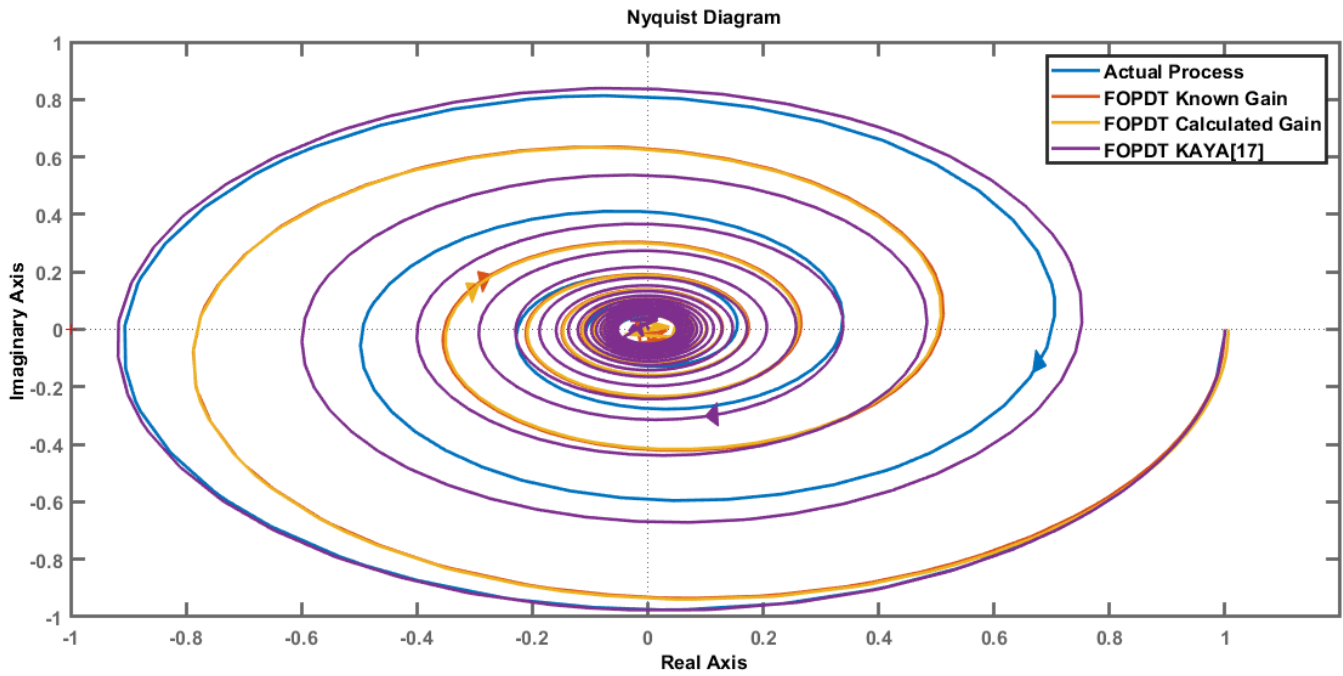


Fig. 6.25: Nyquist Plot of FOPDT for Example 3

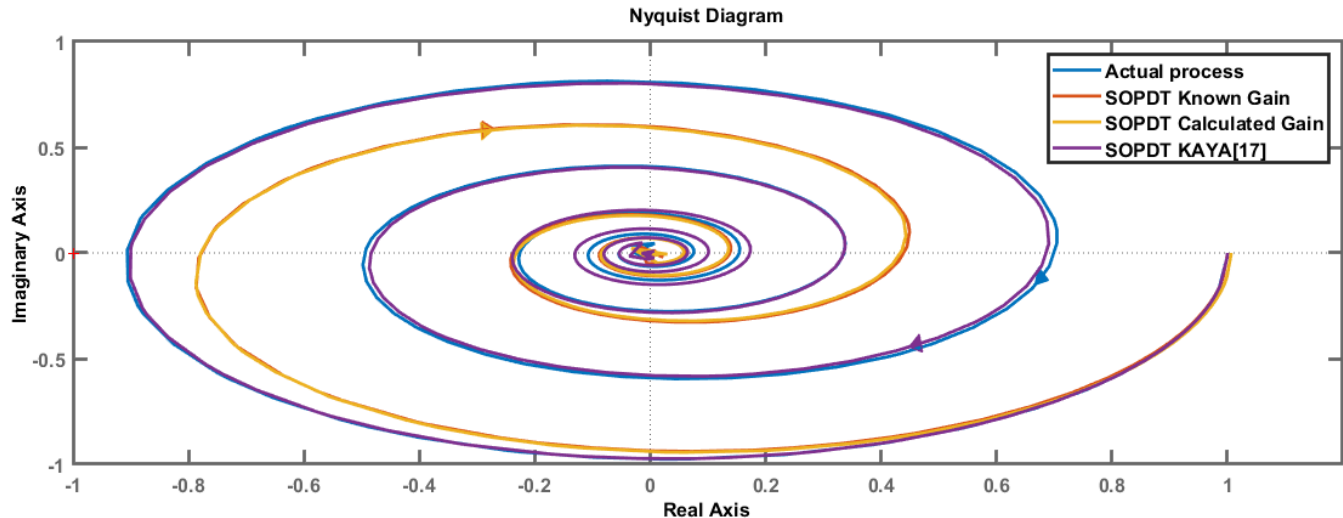


Fig. 6.26: Nyquist Plot of SOPDT for Example 3

The Nyquist plots (refers to Fig. 6.25 & Fig. 6.26) demonstrate a strong resemblance between the Actual Process, the FOPDT model described in reference [17], and the identified FOPDT and SOPDT models. The low IAE values further support the accuracy and reliability of the identified models in representing the Actual Process, making them suitable for practical applications.

6.3.2 Controller design

IMC PID controllers, both fractional-order and integer-order, have been designed for all four process models. The tuning parameter γ , which represents the filter time constant, is chosen based on the

margin of the identified process model's period 'Tu' at which the process becomes marginally stable. In all models, γ is set to 10 per cent of Tu, as indicated in Table 6.10.

Table 6.10: Comparison of filters Example 3

	Integer order	Fractional order
Filter FOPDT known gain	$f_1 = \frac{9.9815s + 1}{50.718s + 25.044}$	$f_1 = \frac{9.9815s + 1}{50.718s^{1.1} + 5.0812s^{0.1} + 19.963}$
Controller FOPDT known gain		$G_c = \frac{6.4410}{0.5} \left(1 + \frac{1}{6.4410s} \right)$
Filter FOPDT calculated gain	$f_1 = \frac{9.946s + 1}{50.528s + 24.972}$	$f_1 = \frac{9.946s + 1}{50.528s^{1.1} + 5.0803s^{0.1} + 19.892}$
Controller FOPDT calculated gain		$G_c = \frac{6.5110}{0.5} \left(1 + \frac{1}{6.5520s} \right)$
Filter SOPDT known gain	$f_1 = \frac{8.7625s + 1}{44.55s + 22.609}$	$f_1 = \frac{8.7625s + 1}{44.55s^{1.1} + 5.0841s^{0.1} + 17.525}$
Controller SOPDT known gain		$G_c = \frac{8.5880}{0.5} \left(1 + \frac{1}{8.5880s} + 2.1470s \right)$
Filter SOPDT calculated gain	$f_1 = \frac{8.709s + 1}{44.272s + 22.502}$	$f_1 = \frac{8.709s + 1}{44.272s^{1.1} + 5.0835s^{0.1} + 17.418}$
Controller SOPDT calculated gain		$G_c = \frac{8.6674}{0.5} \left(1 + \frac{1}{8.7220s} + 2.1805s \right)$
Controller Method in [17] FOPDT model		$G_c = \frac{0.1576}{0.5} \left(1 + \frac{1}{3.67s} \right)$
Controller Method in [17] SOPDT model		$G_C(s) = \frac{0.2636}{0.5} \left(1 + \frac{1}{5.54s} + 1.385s \right)$

Table 6.11: Comparison of IAE, ISE and TV Example 3

		Integer order				Fractional order			
	Tu	p	IAE	ISE	TV	P	IAE	ISE	TV
FOPDT Known gain	5.081	1	38.9674	24.8086	4.8130	1.1	37.6581	24.4459	3.9224
FOPDT Calculated gain	5.080	1	38.8801	24.7320	4.8651	1.1	37.5705	24.3695	3.9632
SOPDT Known gain	5.084	1	34.5923	21.9510	12735	1.1	33.4856	21.6016	430.6171
SOPDT Calculated gain	5.083	1	34.4357	21.8312	13018	1.1	33.3285	21.4822	441.3987
Method in [17] FOPDT model			41.9215	30.1836	1.2000				
Method in [17] SOPDT model			37.8317	27.1276	147.3701				

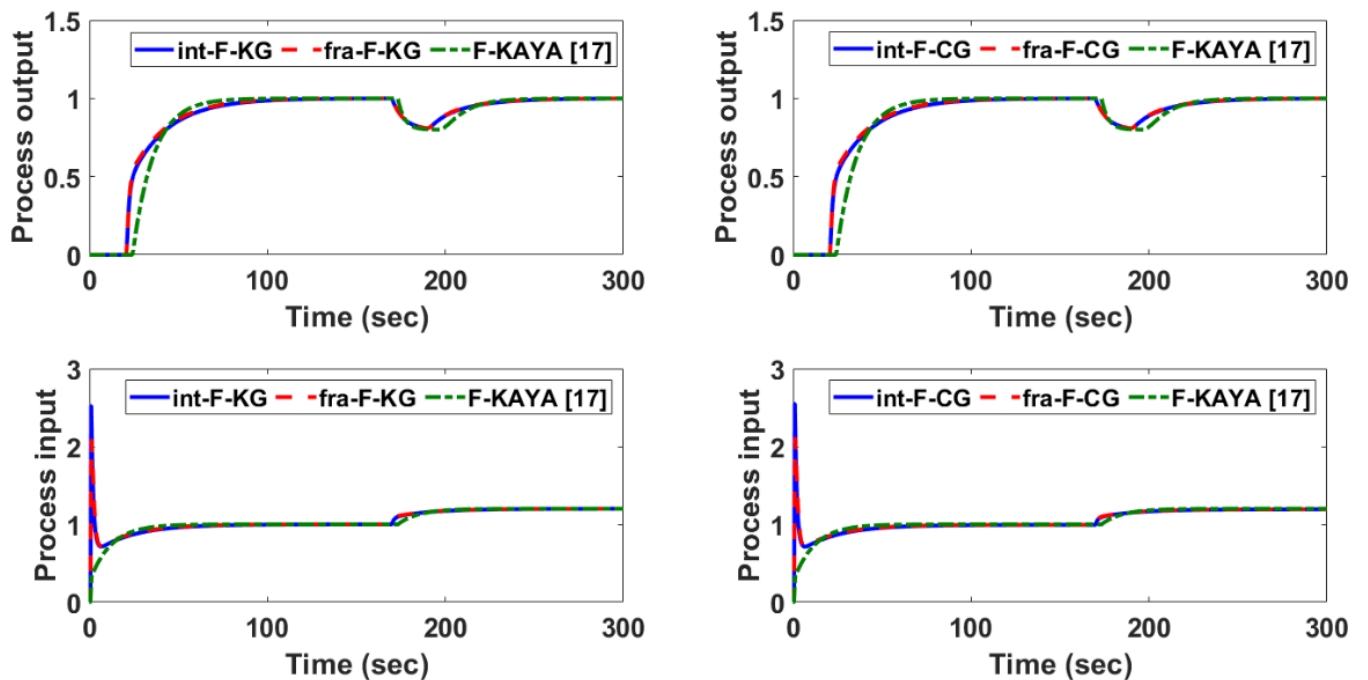


Fig. 6.27: Response of ex. 3 FOPDT Process

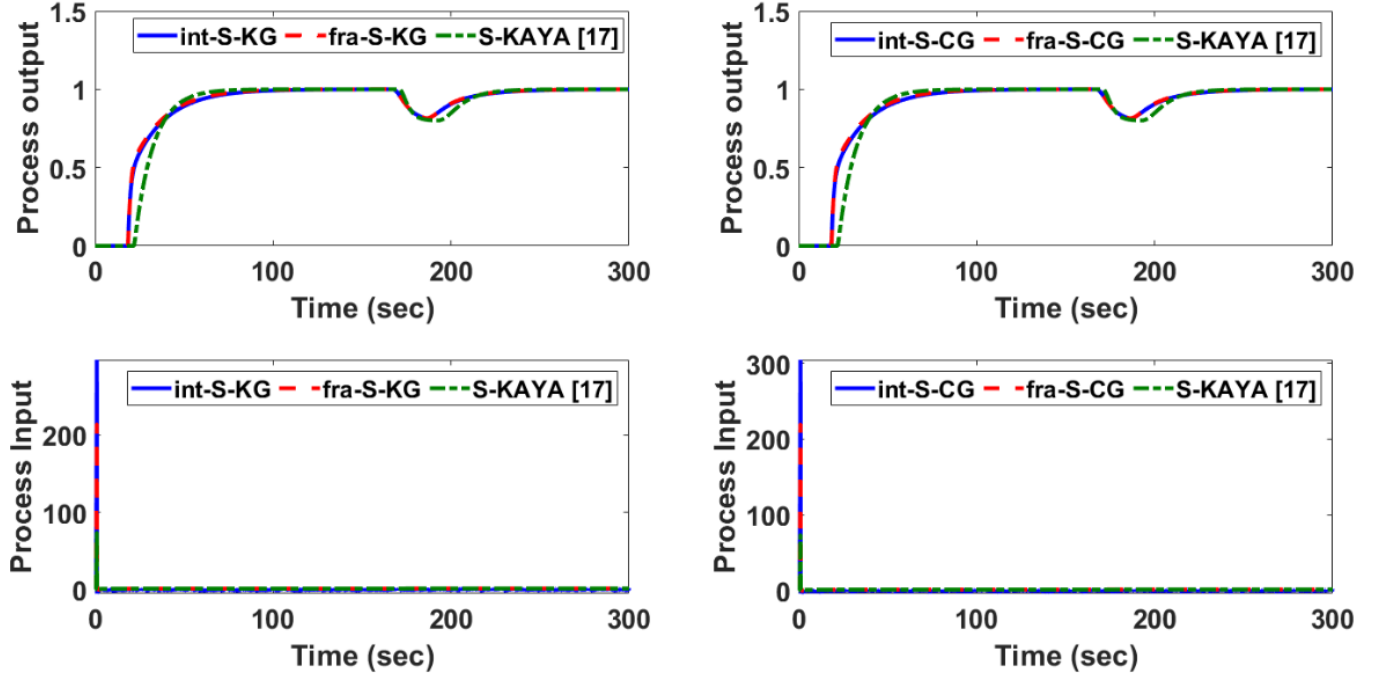


Fig. 6.28: Response of ex. 3 FOPDT Process

Overall, the fractional-order IMC PID controllers exhibit comparable or slightly superior performance compared to their integer-order counterparts in both FOPDT and SOPDT process models, specifically in the IAE, ISE, and TV metrics. The utilization of the calculated gain leads to slightly improved results compared to the known gain, as evidenced by the enhanced IAE and ISE values observed for both the FOPDT and SOPDT models. Moreover, the fractional-order controller consistently outperforms a specific method presented in reference [17] for both the FOPDT and SOPDT models, particularly in terms of the IAE, and ISE metrics. These findings substantiate the overall superiority of the fractional-order IMC PID controllers in terms of their performance (refers to Table 6.11, Fig.6.27 & Fig.6.28).

6.3.3 Robust Analysis

Table 6.12: Performance Criteria for Perturbations in Process Model (Example 3)

Controller		+10% perturbation		-10% perturbation		+20% perturbation		-20% perturbation	
		IAE	TV	IAE	TV	IAE	TV	IAE	TV
FOPDT Known Gain	Integer	38.9849	7.5518	38.9524	7.5269	40.6700	9.9575	38.9788	9.6881
	Fractional	37.8527	7.4197	37.6275	7.4140	40.8688	12.0212	38.0205	11.6489
FOPDT Calculated Gain	Integer	38.8971	7.6307	38.8651	7.6009	40.5624	10.0378	38.8903	9.7290
	Fractional	37.7627	7.4886	37.5392	7.4789	40.7575	12.1129	37.9250	11.6517
SOPDT Known Gain	Integer	34.5991	12582	34.5848	12546	35.7872	12664	34.5870	12516
	Fractional	33.4673	443.105	33.2725	443.158	35.7834	450.559	33.5087	449.880
SOPDT Calculated Gain	Integer	34.4426	13195	34.4287	13081	35.6078	13035	34.4307	12894
	Fractional	33.3101	454.180	33.1165	454.219	35.5901	461.673	33.3489	460.913

FOPDT-Method in KAYA[17]	45.0078	1.3211	41.9017	1.2980	51.0315	1.5612	41.8833	1.4366
SOPDT-Method in I KAYA[17]	40.6156	147.644	37.8236	147.636	46.0876	147.909	37.8146	147.803

After analysing the provided Table 6.12, we can draw the following overall conclusions:

IAE Comparison: The controllers that consistently achieve the lowest IAE (Integral of Absolute Error) values across different perturbations are the SOPDT Calculated Gain Controllers (both Integer and Fractional). They effectively minimize the cumulative error between the desired and actual outputs. The SOPDT Known Gain Controllers (Integer and Fractional) also perform relatively well in terms of IAE, indicating good error reduction. However, all the controllers, including FOPDT (Known Gain and Calculated Gain), demonstrate higher IAE values compared to the SOPDT controllers.

TV Comparison: The controllers that consistently exhibit the lowest TV (Total Variation) values across perturbations are the SOPDT Calculated Gain Controllers (Integer and Fractional). They effectively minimize the variation or change in the control signal, resulting in smoother control. The FOPDT controllers (Known Gain and Calculated Gain) and the SOPDT Known Gain Controllers (Integer and Fractional) show higher TV values compared to the SOPDT Calculated Gain Controllers.

Overall Comparison: Considering both IAE and TV, the SOPDT Calculated Gain Controllers (both Integer and Fractional) are the top performers among the considered controllers. They consistently achieve low IAE and TV values, indicating effective error reduction and smooth control. The SOPDT Known Gain Controllers (Integer and Fractional) also demonstrate favourable performance in terms of IAE, but have higher TV values. The FOPDT controllers (Known Gain and Calculated Gain) generally show higher IAE and TV values compared to the SOPDT controllers.

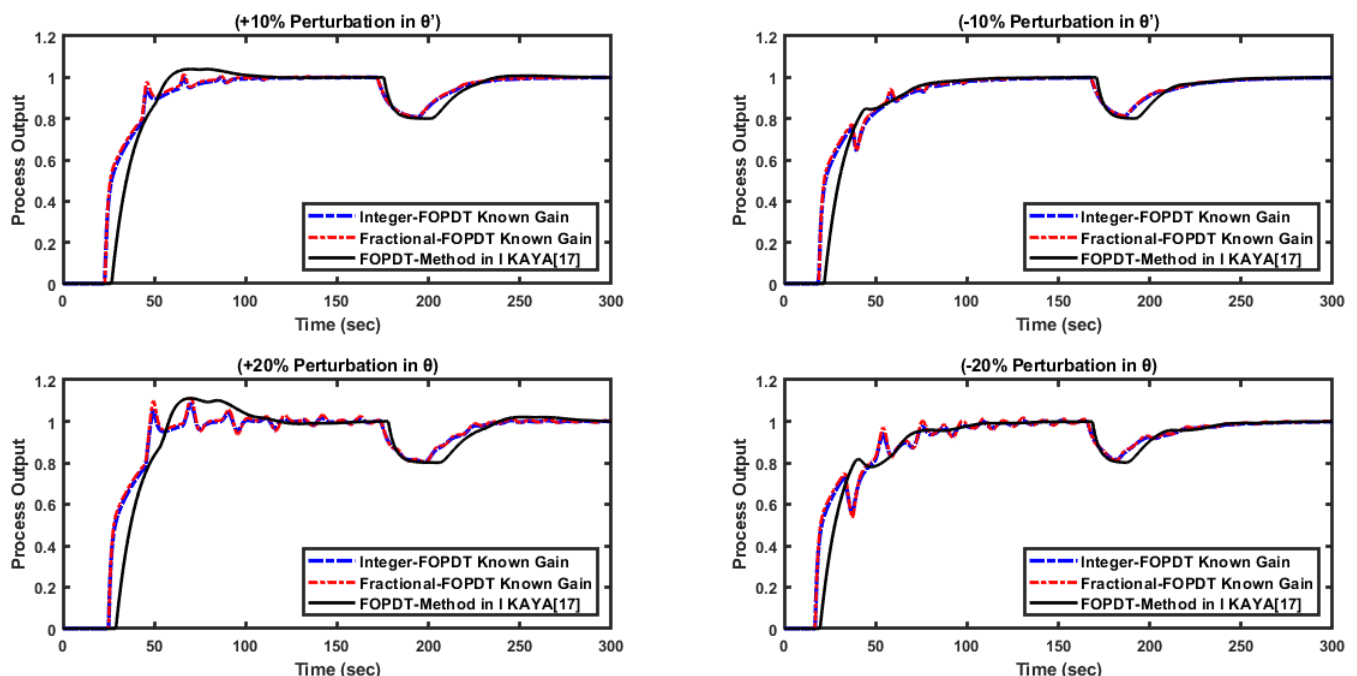


Fig. 6.29: Response of ex.3 for $\pm 10\%$, $\pm 20\%$ change in Time Delay for FOPDT Known Gain

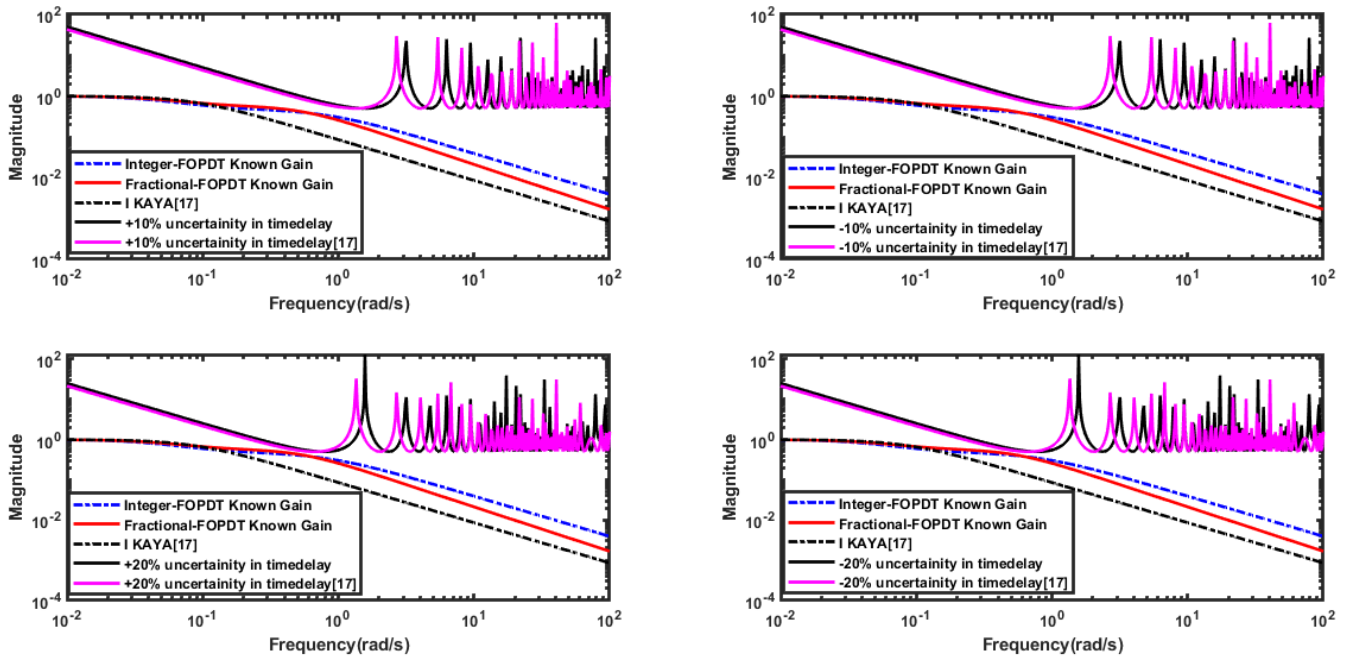


Fig. 6.30: Norm-bound uncertainty of Example 3 for FOPDT Known Gain

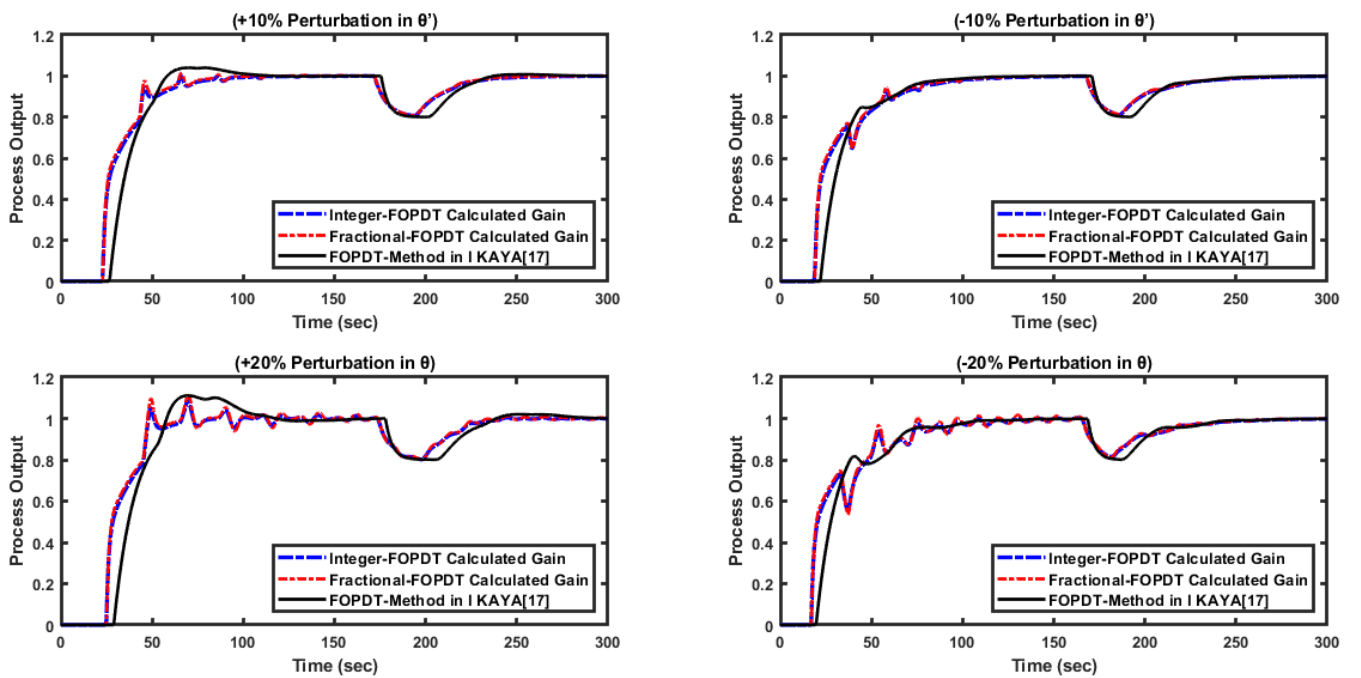


Fig. 6.31: Response of ex.1 for $\pm 10\%$, $\pm 20\%$ change in Time Delay for FOPDT Calculated Gain

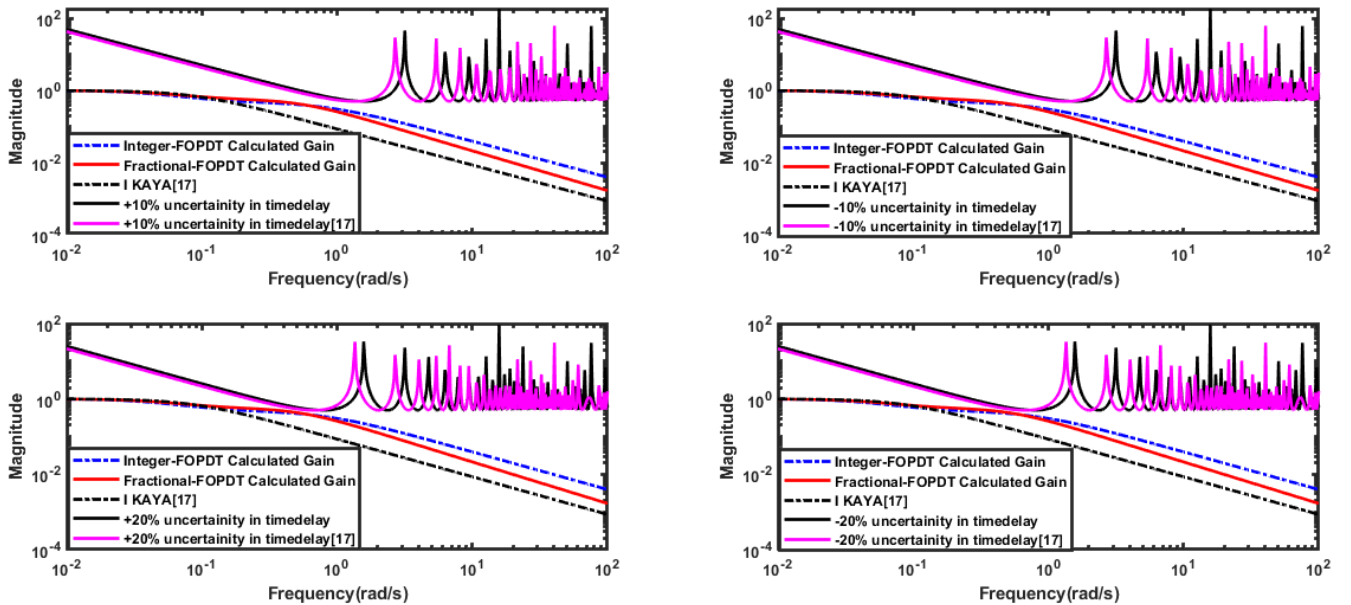


Fig. 6.32: Norm-bound uncertainty of Example 3 for FOPDT Calculated Gain

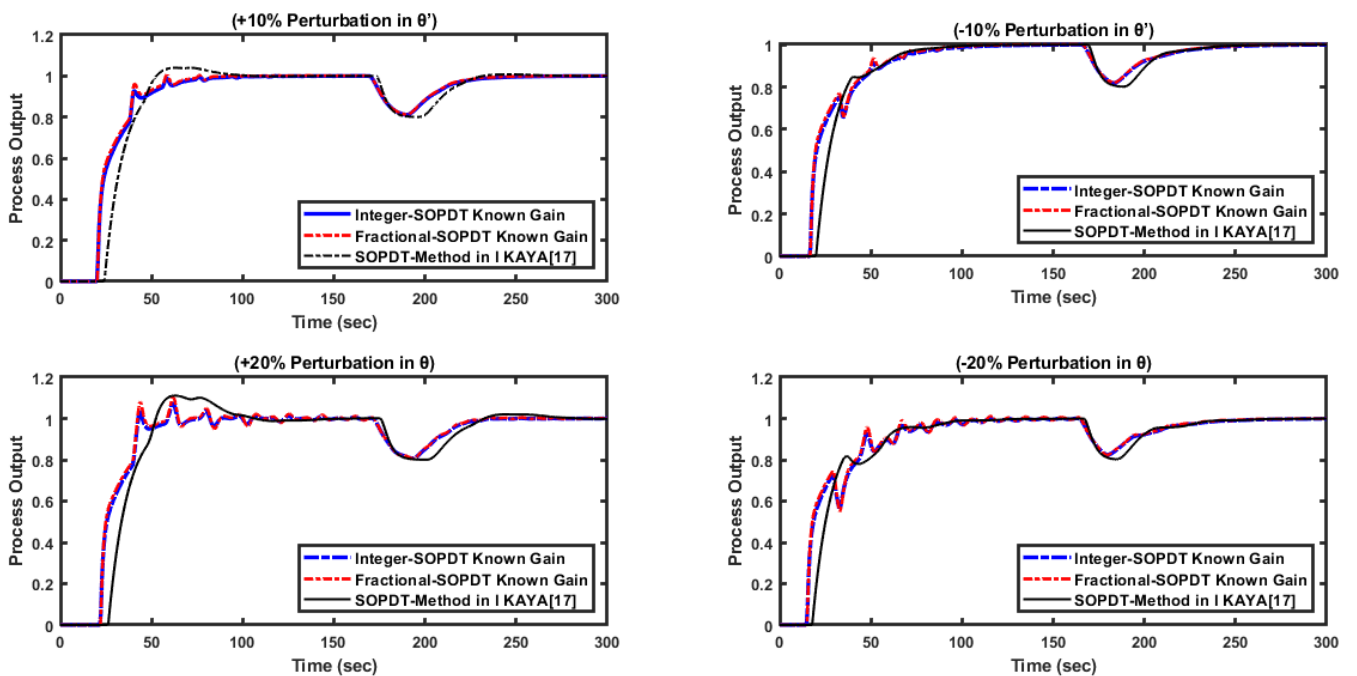


Fig. 6.33: Response of ex.3 for $\pm 10\%$, $\pm 20\%$ change in Time Delay for SOPDT Known Gain

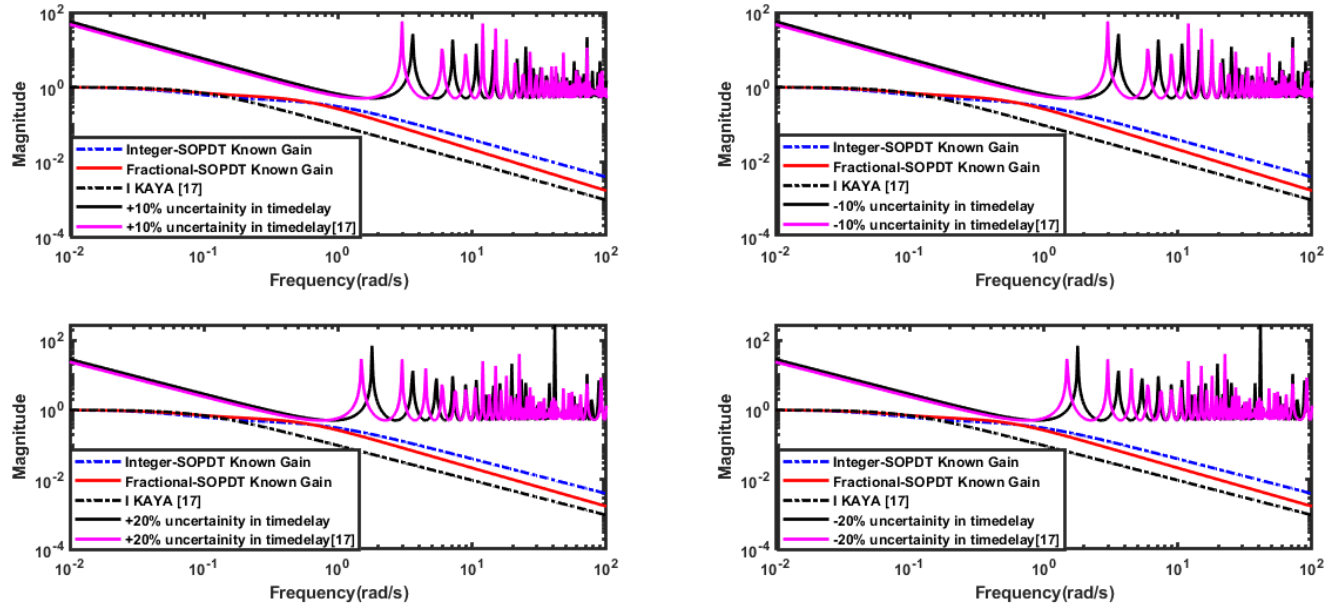


Fig. 6.34: Norm-bound uncertainty of Example 3 for SOPDT Known Gain

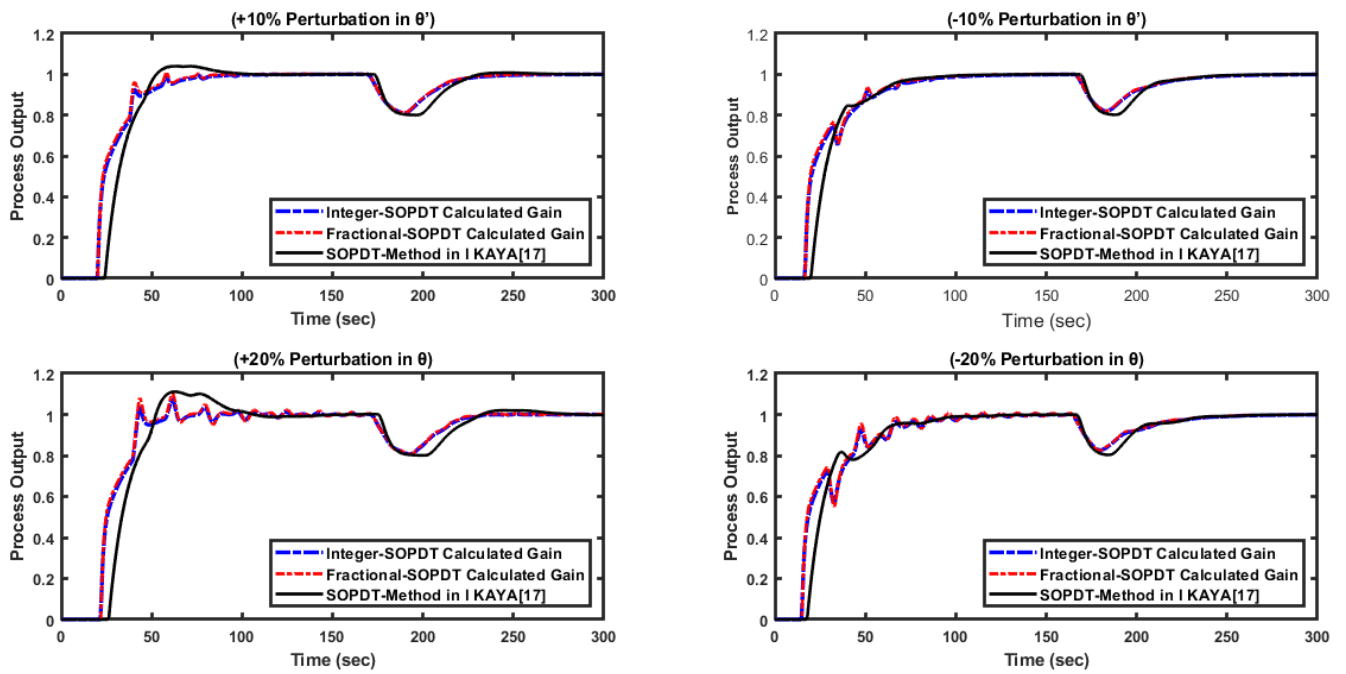


Fig. 6.35: Response of ex.3 for $\pm 10\%$, $\pm 20\%$ change in Time Delay for SOPDT Calculated Gain

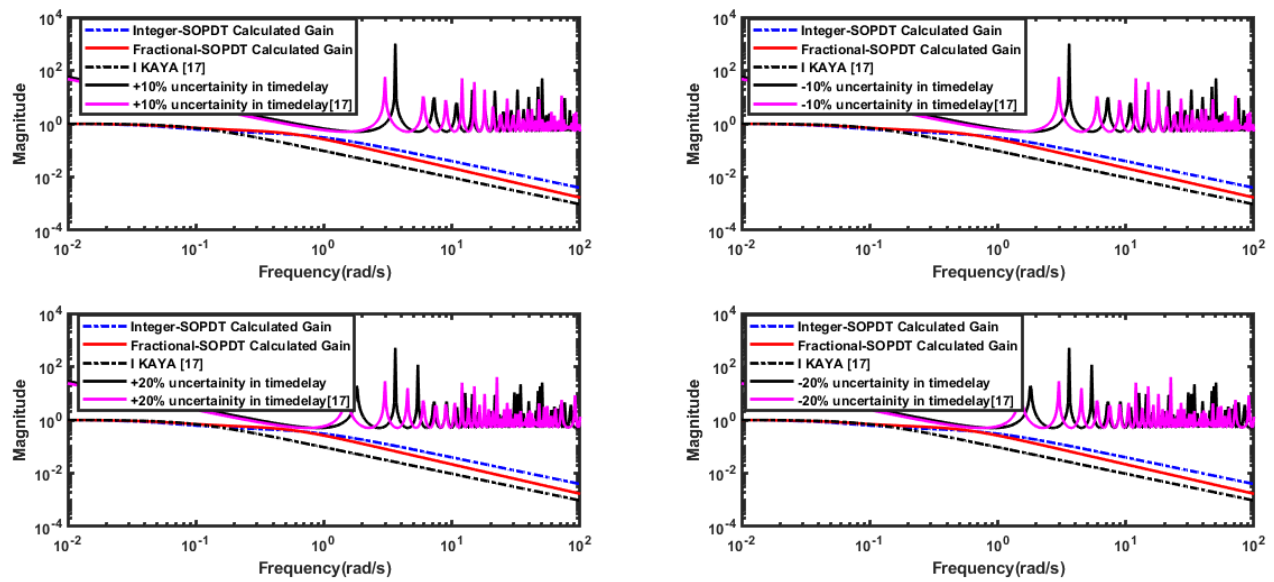


Fig. 6.36: Norm-bound uncertainty of Example 1 for SOPDT Calculated Gain

7. Identification of HO Model & Control for Feedback Configurations

7.1 Identification of HO Models

Proposed identification method applied on following higher order process model

$G_1(s)$, $G_2(s)$, $G_3(s)$, $G_4(s)$, $G_5(s)$ And $G_6(s)$ Taken form literatures [15], [6], [10], [8], [17] and [18] respectively. Identification done by using MATLAB Simulink environment. Relay setting for all examples as $h_1=1.5$, $h_2=-1$ and $\varepsilon = \pm 0.025$, and α is decided based On Error between identified and actual model IAE. The parameters of identified SOPDT Critically damped model of all examples are given in table 7.1.

$$G_1(s) = \frac{0.125e^{-s}}{(s + 1)^3}$$

$$G_2(s) = \frac{1}{(s + 1)^5}$$

$$G_3(s) = \frac{2e^{-8s}}{(7s + 1)^6}$$

$$G_4(s) = \frac{1}{(s + 1)^8}$$

$$G_5(s) = \frac{1}{(s + 1)(0.2s + 1)(0.04s + 1)(0.008s + 1)}$$

$$G_6(s) = \frac{e^{-20s}}{(3s + 1)(2s + 1)(1s + 1)(0.5s + 1)}$$

Table 7.1: Parameters of the identified CSOPDT model

Ex. No.	α	Ap	Av	Tu	K	τ	θ
1	0.5	0.142	0.113	10.9	0.125	1.288	1.526
2	0.8	1.22	0.950	16.4	1	1.763	1.756
3	0.1	2.185	1.573	100	2	13.056	25.413
4	0.1	1.042	0.766	16.2	1	2.220	3.956
5	0.5	0.325	0.322	1.6	1	0.504	0.0181
6	0.1	1.497	0.999	54	1	4.301	17.496

Table 7.2: Comparison of process models

Ex	Methods	Model	IAE
1	Actual Process	$\frac{0.125e^{-s}}{(s + 1)^3}$	--
	Proposed Model	$\frac{0.125e^{-1.526s}}{(1.288s + 1)^2}$	0.0157
	Method in [15]	$\frac{0.124e^{-1.540s}}{(1.281s + 1)^2}$	0.0161
2	Actual Process	$\frac{1}{(s + 1)^5}$	--
	Proposed Model	$\frac{e^{-1.756s}}{(1.763s + 1)^2}$	0.0277
	Method in [6]	$\frac{e^{-1.8011s}}{(1.8605s + 1)^2}$	0.0605
3	Actual Process	$\frac{2e^{-8s}}{(7s + 1)^6}$	--
	Proposed Model	$\frac{2.001e^{-25.413s}}{(13.056s + 1)^2}$	0.0020
	Method in [10]	$\frac{2e^{-22.02s}}{(271.15s^2 + 26.96s + 1)}$	0.0803
4	Actual Process	$\frac{1}{(s + 1)^8}$	--
	Proposed model	$\frac{e^{-3.956s}}{(2.220s + 1)^2}$	0.0136
	Method in [8]	$\frac{e^{-3.36s}}{(2.53s + 1)^2}$	0.0177
5	Actual process	$G_5(s) = \frac{1}{(s + 1)(0.2s + 1)(0.04s + 1)(0.008s + 1)}$	--
	Proposed model	$\frac{e^{-0.0181s}}{(0.504s + 1)^2}$	1.258
	Proposed model	$\frac{e^{-0.232s}}{(1.227s + 1)}$	3.929
	Method in [18]	$\frac{e^{-0.143s}}{(2.65s + 1)}$	7.412
6	Actual process	$G_6(s) = \frac{e^{-20s}}{(3s + 1)(2s + 1)(1s + 1)(0.5s + 1)}$	--
	Proposed model	$\frac{e^{-17.496s}}{(4.301s + 1)^2}$	0.0078

	Proposed model	$\frac{e^{-19.938s}}{(6.453s + 1)}$	0.0078
	Method in [17]	$\frac{e^{-23.28s}}{(3.67s + 1)}$	0.0030

7.2 Controller design

Fractional order filter and IMC PID Controller are design by procedure given section 5.2 tuning parameters and controller performance given in table below Table 7.3.

$$f_1 = \frac{(0.763s + 1)}{0.5213s^{1.02} + 0.6833s^{0.02} + 1.526}$$

$$f_2 = \frac{(0.878s + 1)}{0.7420s^{1.02} + 0.8452s^{0.02} + 1.756}$$

$$f_4 = \frac{(2.611s + 1)}{3.913s^{1.01} + 1.498s^{0.01} + 5.222}$$

$$f_5 = \frac{(0.116s + 1)}{0.0100s^{1.01} + 0.0866s^{0.01} + 0.232}$$

$$f_6 = \frac{(9.969s + 1)}{50.488s^{1.01} + 5.0645s^{0.01} + 19.938}$$

Table 7.3: Controller Design of Identified Higher Order Models

Ex. no.	Methods	α/μ	kc	T _I	T _D	IAE	ISE
1	Proposed		20.60	2.576	0.644	5.0846	3.9012
	Integer IMC	--	20.60	2.576	0.644	5.5611	3.8738
2	Proposed		3.526	3.526	0.8815	6.0295	4.5446
	Integer IMC	--	3.526	3.526	0.8815	6.743	4.550
4	Proposed	1.01/-	3.3750	3.3750	--	8.12	6.31
	Method in [19]	1/1.2	0.33	2.63	2.53	8.95	8.92
5	Proposed	1.01/-	1.2270	1.2270	--	0.373	0.297
	Method in [17]	0.7/-	5.76	1.017	--	0.530	0.290
6	Proposed	1.01/-	6.4530	6.4530	--	43.16	32.02
	Method in[18]	--	0.527	5.540	--	399.00	399.00

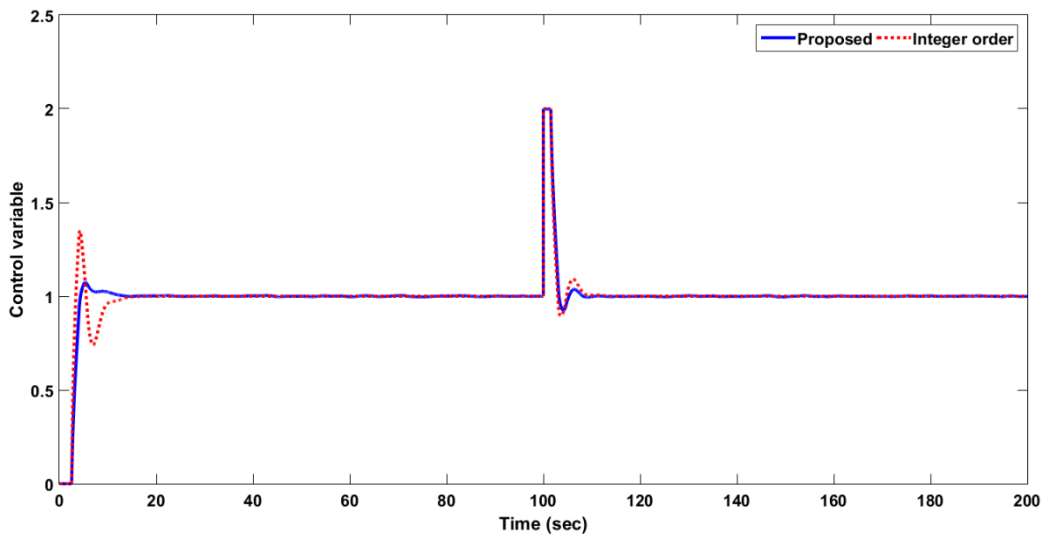


Fig. 7.1: Set-point unit step response for process example 1

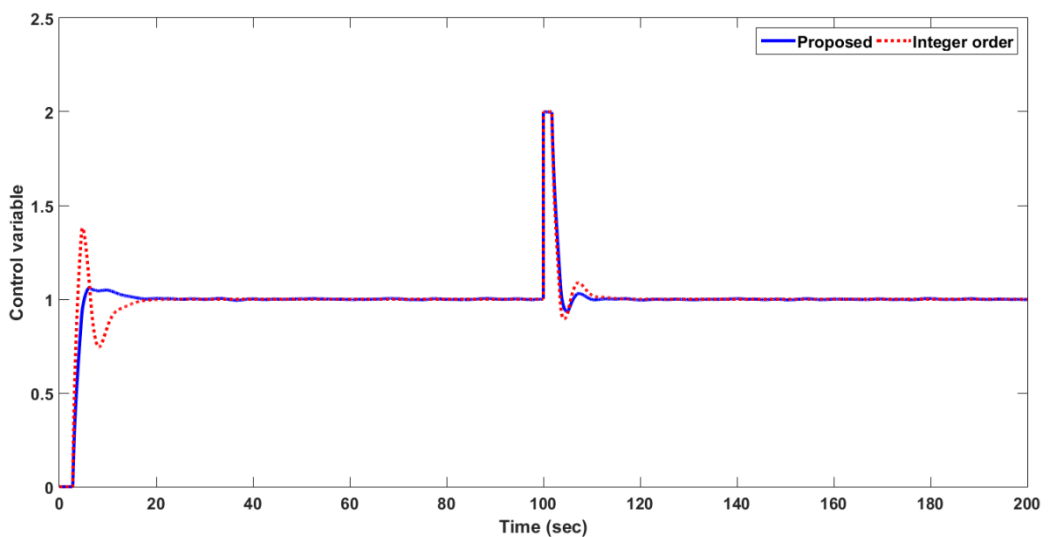


Fig. 7.2: Set-point unit step response for process example 2

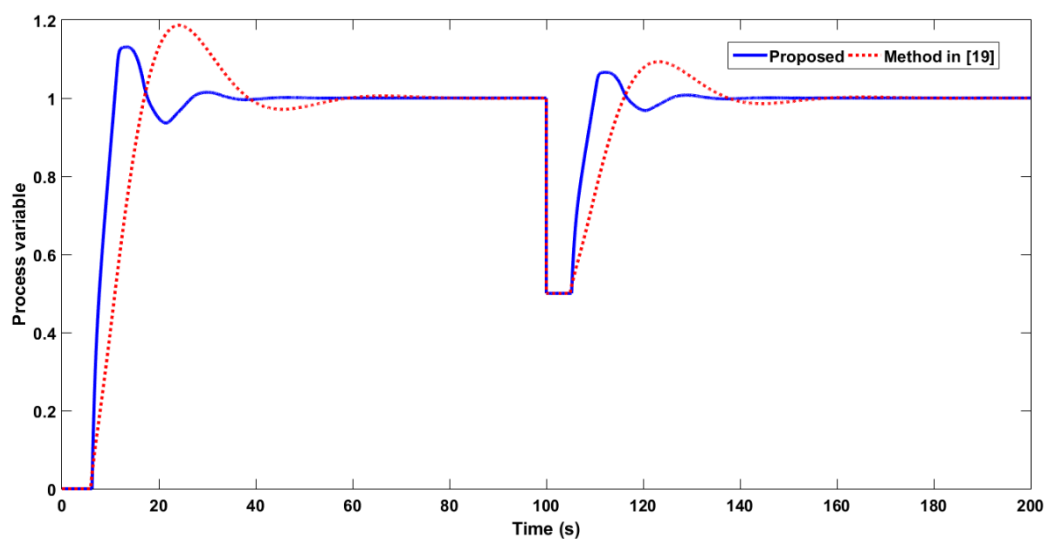


Fig. 7.3: Set-point unit step response for process example 4

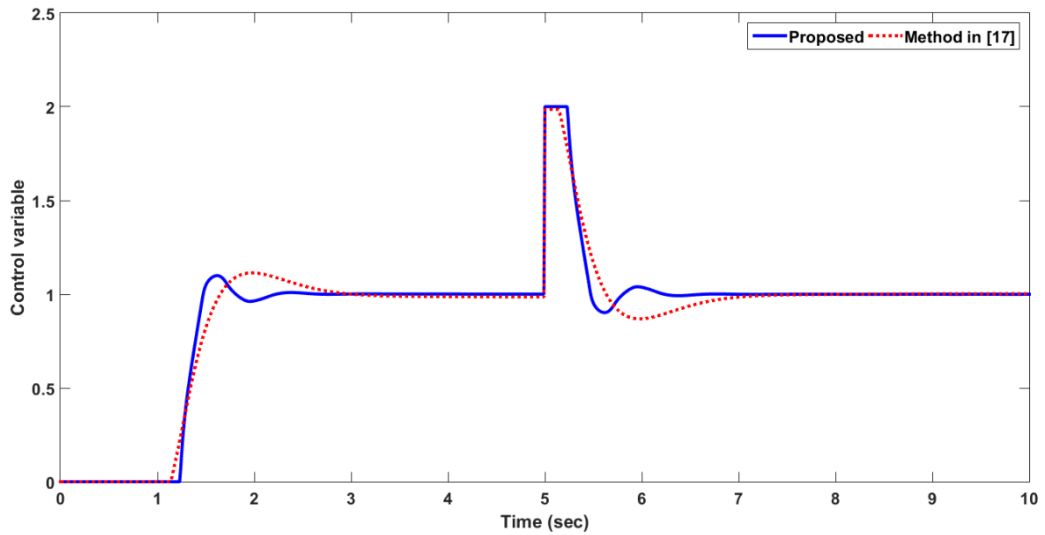


Fig. 7.4: Set-point unit step response for process example 5

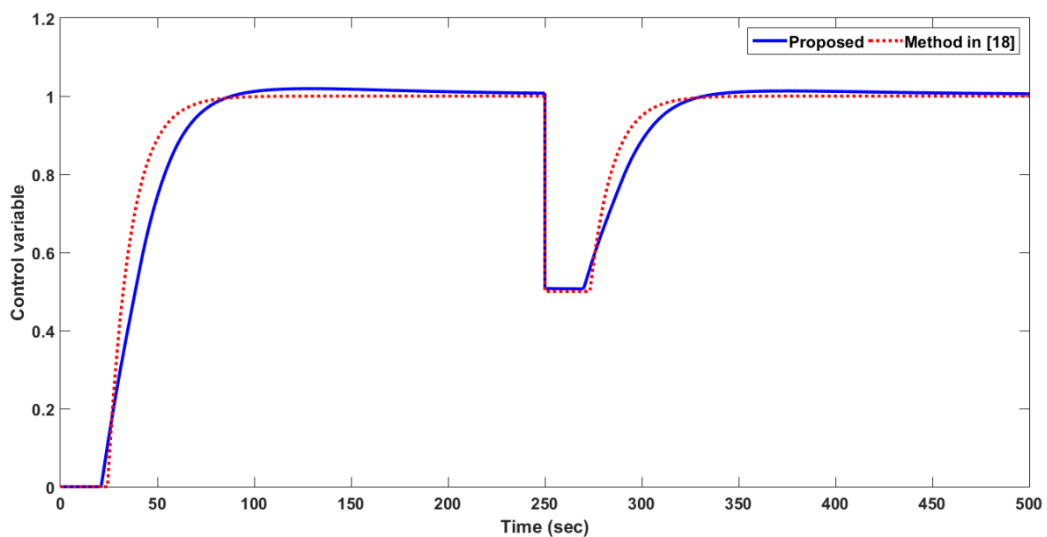


Fig. 7.5: Set-point unit step response for process example 6

By examining Tables 7.2 and 7.3, as well as Figures 7.1-7.5, it can be concluded that the proposed methodology outperforms the reference literature in terms of system identification and closed-loop response in Section 7.

8. Conclusion

In conclusion, this work presents a novel approach for identifying unknown processes using asymmetric relay and fractional order integrators. The proposed method improves the accuracy of FOPDT and CSOPDT models, particularly for higher-order systems. The identified processes are applied in the design of IMC-based PID controllers in Smith predictor and simple feedback configurations. Performance evaluation based on IAE, ISE, and TV criteria demonstrates the superiority of the proposed fractional filter IMC-PID controllers compared to alternative methods. Furthermore, the research suggests that the proposed identification and control design technique can be extended to address unstable processes, investigate unknown process parameters in MIMO systems and Cascade systems, and handle fractional order processes. This study contributes to the advancement of identification and control methodologies with potential applications in various industrial settings.

9. Future Work

The proposed identification and control design technique can be extended to cascade processes, allowing for improved control performance and stability in multi-loop systems.

The proposed identification method can be extended to investigate unknown process parameters of multi-input-multi-output (MIMO) processes, enabling effective control design for complex systems.

The proposed identification and control design technique can be extended to handle fractional order processes, broadening the applicability of the method to systems with non-integer order dynamics.

The proposed identification and control design technique can be extended to address unstable processes, providing a means to stabilize and control systems with inherently unstable behaviour.

After controller tuning, the TV value (total variation) can potentially be reduced by implementing advanced control strategies or techniques beyond the scope of the current project on the control signals.

10. References

- [1] K. J. Astrom, T. Hagglund: Automatic Tuning of Simple Regulators with Specifications on Phase and Amplitude Margins, *Automatica*, Vol. 20, No. 5, 1984, pp. 645-651.
- [2] K. Srinivasan, M. Chidambaram: Modified relay feedback method for improved system identification, *Computer & Chemical Engineering*, Vol. 27, No. 5, 2003, pp. 727-732.
- [3] S. Vivek, M. Chidambaram: Identification using single symmetrical relay feedback test, *Computers and Chemical Engineering*, Vol. 29, No. 7, 2005, pp 1625 – 1630.
- [4] S. Majhi: Relay based identification of processes with time delay, *Journal of Process Control*, Vol. 17, No. 2, 2007, pp. 93 – 101.
- [5] R. Bajarangbali, S. Majhi: Relay Based Identification of Systems, *International Journal of Scientific & Engineering Research*, vol. 3, No. 6, 2012, pp. 1-4.
- [6] P. Ghorai, S. Majhi, S. Pandey: A real-time approach for dead-time plant transfer function modeling based on relay auto tuning, *International Journal of Dynamics & Control*, Vol. 6, No. 3, 2017, pp. 950–960.
- [7] S. Pandey, S. Majhi, P. Ghorai: A new modelling and identification scheme for time-delay systems with experimental investigation: a relay feedback approach, *international journal of systems science*, Vol. 48, No. 9, 2017, pp. 1932-1940.
- [8] S. Narasimha Reddy and M. Chidambaram: Model identification of critically damped second order plus time delay systems, *Indian Chemical Engineer*, Vol 62, No. 1, 2020, pp. 67-77.
- [9] M. Hofreiter: Shifting method for relay feedback identification. *IFAC-Papers Online*, Vol. 49, No. 12, 2016, pp.1933-1938.
- [10] M. Hofreiter: Biased-relay feedback identification for time delay systems, *IFAC-Papers Online*, Vol. 50, No. 1, 2017, pp.14620-14625.
- [11] M. Hofreiter: Alternative identification method using biased relay feedback, *IFAC-Papers Online*, Vol. 51, No. 11, 2018, pp. 891-896.
- [12] M. Hofreiter: Relay feedback identification with additional integral IFAC- Papers Online, Vol. 52, No.13, 2019, pp. 66-71.
- [13] M. Hofreiter: Relay Feedback Identification with Shifting Filter for PID Control, *IFAC Papers Online*, Vol. 54, No. 1, 2021, pp. 498–503.
- [14] P. Ghorai, S. Majhi, V. R. Kasi and S. Pandey: Transfer function identification of a liquid flow-line pressure control system from simple relay auto-tuning, *Transactions of the Institute of Measurement and Control* 2021, Vol. 43, No. 4, 2021, pp. 792–801.

- [15] P. Ghorai, S. Majhi, and S. Pandey: Dynamic model identification of a real-time simple level control system, *Journal of Control and Decision*, 2016, Vol. 3, No. 4, pp. 248-266.
- [16] I. Podlubny: Fractional differential equations, *Mathematics in Science & Engineering*, Academic Press, New York, 1999.
- [17] I. Kaya: IMC based automatic tuning for PID controllers in a Smith predictor configuration, *Journal of process control*, 2004, Vol. 28, pp. 281-290.
- [18] Astrom, K. J., & Hagglund, T. (1995). *PID controllers: Theory, design, and tuning*. Research Triangle Park, NC: ISA.
- [19] Chen, D., & Seborg, D. E. (2002). PI/PID controller design based on direct synthesis and disturbance rejection. *Industrial & Engineering Chemistry Research*, 41, 4807–4822. <https://doi.org/10.1021/ie010756m>
- [20] Dey, C., & Mudi, R. K. (2009). An improved auto-tuning scheme for PID controllers. *ISA Transactions*, 48, 396–409. <https://doi.org/10.1016/j.isatra.2009.07.002>
- [21] Jeng, J.-C., Tseng, W.-L., & Chiu, M.-S. (2014). A one step tuning method for PID controllers with robustness specification using plant step-response data. *Chemical Engineering Research and Design*, 92, 545–558. <https://doi.org/10.1016/j.cherd.2013.09.012>
- [22] Lazarević, M. P. (2006). Finite time stability analysis of PD α fractional control of robotic time-delay systems. *Mechanics Research Communications*, 33, 269–279. <https://doi.org/10.1016/j.mechrescom.2005.08.010>
- [23] Lee, J., Cho, W., & Edgar, T. F. (2013). Simple analytic PID controller tuning rules revisited. *Industrial & Engineering Chemistry Research*, 53, 5038–5047.
- [24] Lee, Y., Park, S., Lee, M., & Brosilow, C. (1998). PID controller tuning for desired closed-loop responses for SI/SO systems. *AICHE Journal*, 44, 106–115. [https://doi.org/10.1002/\(ISSN\)1547-5905](https://doi.org/10.1002/(ISSN)1547-5905)
- [25] Maciejowski, J. M. (1989). *Multivariable feedback design*, Electronic Systems Engineering Series. Wokingham: Addison-Wesley.
- [26] Madhuranthakam, C., Elkamel, A., & Budman, H. (2008). Optimal tuning of PID controllers for FOPDT, SOPDT and SOPDT with lead processes. *Chemical Engineering and Processing: Process Intensification*, 47, 251–264. <https://doi.org/10.1016/j.cep.2006.11.013>
- [27] Morari, M., & Zafiriou, E. (1989). *Robust process control*. Englewood Cliffs, NJ: Prentice Hall.
- [28] Panda, R. C., Yu, C.-C., & Huang, H.-P. (2004). PID tuning rules for SOPDT systems: Review and some new results. *ISA Transactions*, 43, 283–295. [https://doi.org/10.1016/S0019-0578\(07\)60037-8](https://doi.org/10.1016/S0019-0578(07)60037-8)

- [29] Ranganayakulu, R., Uday Bhaskar Babu, G, & Seshagiri Rao, A. S. (2016). A comparative study of fractional order PI λ /PI λ D μ tuning rules for stable first order plus time delay processes. *Resource Efficient Technologies*, 2, S136–S152. <https://doi.org/10.1016/j.reffit.2016.11.009>